Einfluss der Objekterkennung auf die neuronalen Prozesse der Steuerung von Greifbewegungen

Inaugural-Dissertation

zur Erlangung des Doktorgrades

der Medizin

der Medizinischen Fakultät

der Eberhard Karls Universität

zu Tübingen

vorgelegt von

Sheygal, Evgeny

2016

Dekan: Professor Dr. I. B. Autenrieth

1. Berichterstatter: Professor Dr. Dr. H.-O. Karnath

2. Berichterstatter: Professor Dr. H. Wilhelm

Table of Contents

TABLE OF CONTENTS I

ABBREVIATIONS III

1. ZUSAMMENFASSUNG 1

2. SUMMARY 3

3. INTRODUCTION 5

3.1 A window to the outside world: the human visual system 5
3.1.1 Functional organisation of the retina 6
3.1.2 Visual information processing within the geniculostriate pathway 7
3.1.3 Cortical organisation of higher visual processing 8
3.1.4 Vision into movement: the neural basis of target oriented grasping 10
3.1.5 Linking perception and action: the impact object recognition on human grasping 12

3.2 Magnetic resonance as a tool for functional imaging of the human brain 14
3.2.1 Magnetic resonance imaging 14
3.2.2 Blood oxygenation level dependent functional MRI 15
3.2.3 Echo planar imaging 16
3.2.4 Blocked and event related fMRI experimental design paradigms 16
3.2.5 Difficulties of motor studies in fMRI 17

3.3 Aims of this study 19

4. MATERIALS AND METHODS 20

4.1 Reach to grasp movement fMRI study experimental design 20
4.1.1 Participant recruitment 20
4.1.2 Experimental stimuli categories and presentation properties 20
4.1.3 Experimental setup 22
4.1.4. Experimental procedure 25

4.2 Functional and anatomical MRI image acquisition 29
4.2.1 Scanner model and functional volumes imaging specifications 29
4.2.2 Anatomical volumes imaging specifications 29

4.3 Hand movement and eye movement recording 30
4.3.1 Eye movement video recording 30
4.3.2 Hand movement video recording 30

4.4 FMRI data analysis pipelines 32
4.4.1 FMRI data preprocessing 32

4.4.2 Standard approach without kinematics integration 33
4.4.3 Balancing the included trials with regard to a kinematic parameter approach 34
4.4.4 Reach to grasp kinematics as covariates of no interest approach 36
4.4.5 Region of interest extraction 38

5. RESULTS 39

5.1 Effect of object category on reach to grasp kinematics 39

5.2 Evaluation of strategies to incorporate kinematics into the fMRI analysis 41
5.2.1 The standard approach without kinematics integration within the analysis 41
5.2.2 Balancing the included trials with regard to a kinematic parameter approach 42
5.2.3 Including grasp kinematics as covariates into the random effects analysis 45
5.2.4 Strategy evaluation summary 48

5.3 FMRI task related activations contrasted to the baseline signal 50
5.3.1 FMRI activation patterns shown in the attentive viewing task 50
5.3.2 FMRI activation patterns shown in the grasping task 50

5. 4 FMRI signal contrasted between the familiar and geometric categories 53
5.4.1 Impact of object category on the fMRI response during the attentive viewing task 53
5.4.2 Impact of object category on the fMRI response during the grasping task 53

5.5 A closer look at the object category dependent responses 55

6. DISCUSSION 59

6.1 Kinematics incorporation strategies in fMRI 59

6.2 Correlates of object recognition in the human brain 61

6.3 The role of brain areas LOC, aIPS and PMv in visually guided grasping 63

7. CONCLUSIONS 66

8. REFERENCES 67

PUBLICATIONS 76

ERKLÄRUNGEN ZUM EIGENANTEIL 77

Abbreviations

ACC	anterior cingulate cortex
AIP	anterior intraparietal
aIPS	anterior intraparietal sulcus
BOLD	blood oxygenation level dependent
PMd	dorsal premotor cortex
EPI	echo planar imaging
TE	echo time
FAM	familiar objects
FWE	familywise error rate
FOV	field of view
FWHM	full width at half maximum
fMRI	functional magnetic resonance imaging
GLM	general linear model
GEO	geometric objects
HRF	haemodynamic response function
HF-Pulse	high frequency pulse
LGN	lateral geniculate nucleus
LOC	lateral occipital cortex
LED	light-emitting diode
MR	magnetic resonance
MRI	magnetic resonance imaging
MFG	middle frontal gyrus
MNI	Montreal Neurological Institute
MT	movement time
ROI	region of interest
TPJ	temporoparietal junction
TR	repetition time
RT	response time
SEM	standard error of the mean
SPM	statistical parametric maps
SPL	superior parietal lobule
PMv	ventral premotor cortex

1. Zusammenfassung

Das zielgerichtete Ergreifen bildet beim Menschen eine wesentliche Grundlage der Interaktion mit unserer Umwelt und somit des selbstständigen Lebens. Gleichzeitig stellt dieser Vorgang hohe Anforderungen an die zentralnervöse Verarbeitung: das erwünschte Ziel muss unter vielen möglichen Alternativen ausgewählt werden, seine Größe und räumliche Lage aus der visuellen Information ermittelt, und der Erstellung eines motorischen Programms zugeführt werden. Dabei gelingt dem gesunden Menschen eine fließende Bewegung mit adäquater Handformung, objektbezogener Griffskalierung und genau dosiertem Krafteinsatz. Die Untersuchung der neuronalen Grundlagen des visuell gesteuerten Ergreifens beim Gesunden bildet daher eine unverzichtbare Grundlage zum Verständnis von neurologischen Krankheitsbildern, die mit einer Einschränkung dessen einhergehen. Eine dieser Störungen ist die optische Ataxie. Patienten mit einer optischen Ataxie zeigen Defizite im zielgerichteten Ergreifen von Gegenständen, bei vorhandener Fähigkeit diese Gegenstände zu erkennen und zu beschreiben (Jakobson, Archibald, Carey, & Goodale, 1991; Jeannerod, 1986). Ein gängiges Modell (M. A. Goodale & Milner, 1992) erklärt dieses Verhalten mit der dualen Dissoziation der visuellen Informationsverarbeitung in zwei größtenteils voneinander unabhängige Verarbeitungsströme. Der ventrale okzipitotemporale Strom dient der Erkennung von Objekten, während der dorsale okzipitoparietale Strom, nur anhand von visuell feststellbaren physikalischen Eckdaten, wie Größe und Entfernung der Objekte, zur Steuerung und Planung des motorischen Ergreifens dient. In einer Fallstudie (Jeannerod, Decety, & Michel, 1994) zeigte sich jedoch, dass eine Patientin mit optischer Ataxie ihr bekannte Gegenstände, wie z.B. einen Lippenstift, präziser ergreifen konnte als abstrakte zylindrische Objekte. Eine naheliegende Folgerung ist, dass die Identifikation bekannter Gegenstände maßgeblich in die zerebralen Prozesse der Greifbewegungssteuerung einfließen muss.

Im Rahmen unserer fMRT Studie haben gesunde junge Probanden bei laufender funktioneller Magnetresonanzmessung nach bedeutungsvollen

Alltagsgegenständen, wie z.B. einem Textmarker oder einer Streichholzschachtel, und assoziationsfreien einfarbigen Holzblöcken griffen. Dabei wurde der komplette Bewegungsablauf mit 2 MR-kompatiblen Kameras aufgezeichnet und auf kinematische Basisparameter wie Reaktionszeit, Bewegungszeit etc. untersucht. In einer methodologischen Untersuchung konnten wir eine deutliche Auswirkung der Inklusion dieser Basisparameter in die funktionelle Ganzgehirnanalyse feststellen und eine geeignete Strategie zur Integration dieser Parameter in die fMRT-Analyse finden. Die darauffolgende vergleichende Analyse des visuell gesteuerten Ergreifens ergab höhere Signalunterschiede in den Gehirnarealen lateraler okzipitaler Kortex (LOC), anteriorer intraparietaler Sulcus (aIPS) und ventraler prämotorischer Kortex (PMv) beim Ergreifen von bedeutungsvollen Alltagsgegenständen im Vergleich zum Ergreifen von in ihren physikalischen Dimensionen zu den Alltagsgegenständen passenden einfarbigen Holzblöcken. Bei der aufmerksameren Betrachtung der beiden Objektkategorien konnten wir stärkere Signale beim Betrachten der Alltagsgegenstände im Vergleich zum Betrachten der Holzblöcke nur im LOC feststellen. In den Regionen aIPS und PMv wurden bei der aufmerksamen Betrachtung keine signifikanten Signalunterschiede gefunden. Somit konnten wir den LOC erwartungsgemäß als maßgeblich in der Objekterkennung involviertes Areal sowohl beim aufmerksamen Ansehen als auch beim visuell gesteuerten Ergreifen feststellen. Währenddessen stellten sich, anders als ausgehend vom Modell von Goodale und Milner (1992) zu erwarten wäre, aIPS und PMv als greifrelevante Areale dar, die zur Integration der aus der Objekterkennung hervorgegangenen erfahrungsbasierten Informationen in die motorische Planung des Ergreifens beitragen.

2. Summary

Target oriented grasping forms a crucial basis for human-environment interaction, and is essential for autonomous living. At the same time the process of visually guided grasping imposes high demand on the central nervous system: the desired target object has to be identified and chosen among a high number of alternative targets; based on visual input its size and position in space has to be determined, and made available for the motor command formation. Despite this complexity, healthy humans effortlessly perform fluid grasping movements with adequate hand shaping, object oriented grip scaling and exact employment of force. The study of visually guided grasping and its neuronal underpinnings, in healthy participants, can contribute tremendously to the understanding of neurological disorders associated with grasp deficits. An impressive example is optic ataxia. Patients with optic ataxia show deficits in target oriented reaching and grasping, with an intact ability to identify and describe objects presented to them (Jakobson et al., 1991; Jeannerod, 1986). A popular model (M. A. Goodale & Milner, 1992) explains this behavior with the dual dissociation of visual information processing in two essentially independent processing streams. The ventral occipitotemporal stream is involved in perception and object identification, while the dorsal occipitoparietal stream uses only visually accessible physical object properties, like its size and position in order to plan and execute reach to grasp movements. However, a case study could demonstrate that a patient with optic ataxia could grasp objects familiar to her, for example a lipstick, with greater precision than abstract cylindrical forms (Jeannerod et al., 1994). A plausible conclusion is, that object recognition contributes substantially to the cerebral processes of grasp control.

In our fMRI experiment, healthy young participants performed reach to grasp movements toward meaningful everyday objects, like a text highlight pen or a matchbox, and association free unicolour wooden blocks of matched physical dimensions. Reach to grasp actions were recorded using two MR compatible video cameras and analysed for basic kinematic parameters (e.g. response time and movement time). In a methodological investigation we demonstrated

the impressive influence of the inclusion of kinematics into the whole brain functional analysis, and determine an appropriate strategy of kinematics incorporation in form of employing them as covariates in the group level analysis. The differential analysis of visually guided grasping revealed stronger signal within the lateral occipital cortex (LOC), the anterior intraparietal sulcus (aIPS) and the ventral premotor cortex (PMv) during the planning of reach to grasp movements towards meaningful everyday objects compared to grasping towards unicolour wooden blocks. Attentive viewing of the meaningful objects led to higher signal levels in the LOC as compared to attentively viewing the wooden blocks. No significant signal differences could be detected between the two purely visual conditions in the brain areas aIPS and PMv. Thus we could identify the LOC as a critical area of object recognition during both attentive viewing and visually guided grasping, as expected. Contrary to what we expected based on the model of Goodale and Milner (1992), the dorsal stream areas aIPS and PMv act as grasp specific regions, that contribute to the integration of object recognition and thus experience-based object information in motor grasp planning.

3. Introduction

The process of visually guided grasping imposes high demand on the central nervous processing: the desired target object has to be identified and chosen among a high number of alternative targets; based on visual input its size and position in space has to be determined, and made available for the motor command formation. Despite this complexity, healthy humans effortlessly perform fluid grasping movements with adequate hand shaping, object oriented grip scaling and exact employment of force.

3.1 A window to the outside world: the human visual system

The human eye is an impressive organ with the distinctive ability to detect electromagnetic radiation with the wavelength between 400nm and 750nm (visible light) as its appropriate stimulus. Light passes through the refractory system consisting of the lens, cornea and the vitreous body onto the retina where it is being encoded into neuronal signals, eventually converging within the optic nerve. The eye's optical axis runs through the fovea centralis, a pit of approx. 1,5mm diameter with the greatest density of light receptor cells. The exit site of the optic nerve is located nasal to the fovea centralis, and is not covered by light receptor cells, therefore presenting a natural blind spot. While visual afference from the optic nerve is divergently connected to numerous diencephalic (lateral geniculate nucleus, suprachiasmatic nucleus), cerebral (primary visual cortex) and brainstem (superior colliculus) areas, the geniculostriate pathway of visual information through the optic nerve across the optic chiasm to the lateral geniculate nucleus and from there via the optic radiation to the primary 'striate' visual cortex is considered the dominant visual pathway in mammals, and is essential for the formation of conscious vision in humans (Halperin, 2009; Schmidt, Lang, & Thews, 2007).

3.1.1 Functional organisation of the retina

There are two types of light receptor cells within the retina, namely rods and cones. The rods are most sensitive to wavelengths around 498nm, have their highest density in the parafoveal zone, and are easily blinded under illumination levels above 1 cd/m² due to their low excitation threshold, thus being mainly responsible for low light scotopic vision (Wandell, 1995). The cones exist in 3 variants most sensitive to wavelengths of 420nm, 535nm and 565nm respectively (Stockman, MacLeod, & Johnson, 1993), thereby allowing colour discrimination, have their highest density in the fovea centralis, and are the dominant receptor cells under luminance levels between 1 and 10^6 cd/m² (photopic vision). The transformation of a light stimulus into neuronal signals, known as visual phototransduction, is initiated by light quanta triggering a stereoisomerisation of 11-cis-retinal to all-trans-retinal as the first step of a biochemical cascade resulting in cell hyperpolarisation and successive decrease of glutamate neurotransmitter release by the light receptor cells; for review see (Ebrey & Koutalos, 2001; Lagnado & Baylor, 1992; Tranchina, 1998). In the case of cones, this decrease of glutamate release leads to depolarisation of ON-bipolar cells and hyperpolarisation of OFF-bipolar cells, which exhibit synaptic connection to ON ad OFF ganglion cells respectively, leading to a depolarisation in ON and hyperpolarisation in OFF ganglial cells (Jonas & Memorial, 1970). In the case of rods, a detour is taken: decreasing glutamate release leads to depolarisation of rod bipolar cells that excite rod amacrine cells, that in turn depolarise ON bipolar cells via an electric and inhibit OFF bipolar cells via a chemical synapse. Thus, rod excitation has a similar effect on the ON and OFF ganglial cells as cone excitation. For more details on mammal retina architecture see Wässle & Boycott (1991).

Ganglion cells exhibit inhibitory connections to the surrounding ganglion cells, forming antagonising circular receptive fields. Therefore medial illumination of a ganglion cell's receptive field leads to inhibition of surrounding ganglion cells, a mechanism considered fundamental for visual contrast detection (Kuffler, 1953; Robson, 1966). Further investigation of retinal ganglion cell properties revealed 2 dominant neuron types: the colour sensitive X cells with small receptive fields

(meaning high spatial resolution) and intermediately fast conducting axons, and the colour insensitive Y cells with large receptive fields and fast conducting axons (Dreher, Fukada, & Rodieck, 1976; Humphrey, 1970; Lennie, 1980). This dichotomy provides a first indication for the existence of specialized visual pathways in mammals.

3.1.2 Visual information processing within the geniculostriate pathway

Interestingly the subdivision of visual information pathways is also apparent not only in the retina, but also in subsequent stations of the geniculostriate visual pathway. The lateral geniculate nucleus (LGN), an essential diencephalic node of the mammal visual pathway, has four dorsal parvocellular layers and two ventral magnocellular layers, with each eye projecting to 3 of the 6 layers. Hereby the parvocellular and magnocellular layers of LGN gain their afference from distinct populations of retinal ganglion cells (Leventhal, Rodieck, & Dreher, 1981). Parvocellular LGN neurons are predominantly (~90%) colour sensitive, have a smaller receptive field, slower response time and less contrast sensitivity than magnocellular LGN neurons. Magnocellular LGN neurons on the other hand are insensitive to differences in wavelength, have a larger receptive field, respond faster and are sensitive to low contrast stimuli (Livingstone & Hubel, 1988).

When traced further into the primary visual area V1 the abovementioned LGN layers exhibit different projection pathways. The magnocellular LGN layers project into V1 layer 4Cα, which projects into layer 4B. Neurons in layer 4B are orientation selective, movement direction selective and indiscriminate to colours (Dow, 1974). Projections from layer 4B include secondary visual area V2 and the medial temporal lobe.

Parvocellular LGN layers on the other hand side project into layer 4Cβ, which projects into layers 2 and 3, particularly into cytochrome oxidase stainable ‘blobs’ and unstainable ‘interblobs’ (Hendrickson, Hunt, & Wu, 1981; Tootell, Hamilton, & Silverman, 1985). The interblob neurons are orientation selective,

have small receptive fields, and are not explicitly colour selective, but sensitive for contrast borders, therefore possibly being involved in high resolution form perception (Livingstone & Hubel, 1988). Blob cells are either brightness or colour coded, and might present an early correlate for colour and pattern analysis. Blob and interblob regions further project into V2 and V4.

So far we have been able to distinguish the cellular basis of two distinct components of visual information processing: a parvocellular system capable of colour discrimination and high resolution shape analysis, and a magnocellular system that is insensitive to colour and has a lower resolution, but is responding faster and is sensitive to movement. It must be noted however that the separation is not absolute at V1 level already, for example with the magnocellular system contributing projections to layer 2 and 3 blob areas (Livingstone & Hubel, 1984). Whether this duality perseveres in higher visual areas will be the next topic we shall take a closer look at.

3.1.3 Cortical organisation of higher visual processing

A very influential model of higher visual processing has been introduced by Ungerleider & Mishkin (1983). Based on the finding, that rhesus monkeys with surgical lesions of the inferior temporal cortex perform poorly in object discrimination tasks (Pohl, 1973), while monkeys with lesions of the posterior parietal cortex underperform in a landmark discrimination task, Ungerleider & Mishkin postulated a two stream hypothesis of higher visual processing. This hypothesis states, that spatial visual information is being managed in the dorsal occipitoparietal pathway (‘where-pathway’), while object vision takes place in the ventral occipitotemporal pathway (‘what-pathway’). This model matches well with the finding of magnocellular and parvocellular LGN systems (Livingstone & Hubel, 1988), forming a basis of specialized visual processing at the retinal level and extending via the LGN to the primary and secondary visual areas. While recordings of the medial temporal lobe largely confirm the segregation of magnocellular and parvocellular LGN inputs in higher cortical areas (Maunsell, Nealey, & DePriest, 1990), V4 proved to receive strong input from both subdivisions of the LGN (Won, Lee, & Son, 2008).

The model proposed by Ungerleider et al. (1998) has later been challenged by Goodale and Milner (1992): while the anatomical basis of the ventral and dorsal stream separation remained confirmed (Young, 1992), Goodale and Milner had a different view on the output properties of the systems. In contrast to Ungerleider and Mishkin's model of visual processing seperation into spatial vision and object vision, Goodale and Milner introduced the idea that both spatial and stimulus-quality information is used within both the ventral and the dorsal stream, but for different purposes: the ventral stream constructs a perceptual representation of the visual world while the dorsal stream is involved in visual action control. The authors therefore addressed the dorsal stream as the 'how pathway', while still referring to the ventral stream as the 'what pathway'.

Indications for the functional dissociation of the two aforementioned pathways can be obtained by studying neuropsychological disorders following lesions of either ventral or dorsal stream areas in humans. Patients with lesions including the occipitotemporal region, an area of the ventral stream, exhibit a set of syndromes known as visual form agnosia (Farah, 2004). So far, only two patients with visual form agnosia have participated in neuropsychological investigations (Karnath, Rüter, Mandler, & Himmelbach, 2009; A D Milner et al., 1991). These patients were unable to visually recognize simple objects or geometric shapes as well as faces of friends or relatives. However, when handling visually guided motor tasks, like navigation in familiar settings, or even reach to grasp tasks towards the unrecognized objects, they performed surprisingly well. On the other hand, patients with lesions covering the posterior parietal cortex develop a disorder categorized as optic ataxia (Perenin & Vighetto, 1988). The patients with optic ataxia can generally identify line drawings of everyday items with relative ease (M. A. Goodale et al., 1994), and yet they fail to accurately reach out to target objects or scale their grasp accordingly, and display a large number of correction movements.

3.1.4 Vision into movement: the neural basis of target oriented grasping

Target directed grasping requires the transformation of visually acquired object size and position information into appropriate arm transport, hand shape and grip scaling. So far we had a first look at cerebral visual processing, which appears to be segregated into a ventral occipitotemporal and a dorsal occipitoparietal stream of visual processing. Of the two streams it is the dorsal system that is tightly linked to visual movement control (M. A. Goodale & Milner, 1992), and lesions in the dorsal stream lead to substantial impairments of visually guided grasping leading to incorrect hand preshaping, increased number of correction movements, or even far-reaching deficiency of prehension resulting in awkward palmar grasping (Jakobson et al., 1991; Jeannerod et al., 1994). We shall therefore acquaint ourselves further with the particular areas within the dorsal stream essential for reach and grasp calculation, and their connections to cerebral motor output areas, such as the premotor cortex PM and the primary motor cortex M1.

Critical insights into the neural organisation of visually guided grasping have been procured by neurophysiological studies of nonhuman primates. A key network of grasp related visuomotor transformations in monkeys consists of the directly connected areas F5 within the monkey ventral premotor cortex and the anterior intraparietal sulcus area AIP (Luppino, Murata, Govoni, & Matelli, 1999; Matelli & Luppino, 2001). Both the AIP and F5 code for object related grasping actions, with the AIP representing the complete movement (Murata, Gallese, Luppino, Kaseda, & Sakata, 2000), while F5 focuses on parts of that movement (Murata et al., 1997). Additionally, visually evoked responses to 3-dimensional images could be recorded within the AIP (Murata et al., 2000). Based on these findings Fagg and Arbib (1998) introduced a model according to which the AIP extracts grasp relevant visual information of target objects, while the area F5 selects the corresponding grasp type and manages its execution. The grasp management role of area F5 is enabled by cortico-cortical connections to the primary motor cortex (Stark, Globerson, Asher, & Abeles, 2008), and even

direct connections to the brainstem and spinal cord (Borra, Belmalih, Gerbella, Rozzi, & Luppino, 2010).

Drawing parallels between the monkey and human visual grasp control systems is difficult and controversial. With invasive human brain electrophysiological studies being rightfully unethical, insights into human visuomotor systems are largely based on lesion and imaging studies. A particularly interesting example from Binkofski et al. (1998) demonstrated, that lesions of the human anterior lateral bank of the intraparietral sulcus (human AIP/ aIPS) lead to impairment of grasping, but not reaching. An additional functional MRI experiment procured by the authors compared reaching and grasping a rectangular object to just reaching to it. While general signal patterns during grasping and reaching included contralateral sensorimotor cortex, bilateral premotor cortex, the supplementary motor area, and bilateral posterior parietal cortices, the differential analysis was much more localized revealing stronger signal within the bilateral aIPS in grasping opposed to reaching (Binkofski et al., 1998). A different fMRI grasping study towards an array of unpredictable objects could also demonstrate greater signal in the aIPS during grasping than during reaching (Culham et al., 2003). These results showed that it is at least plausible to regard the aIPS as a human homologue of the monkey AIP. A different fMRI experiment by Grèzes, Armony, Rowe, & Passingham (2003) showed activations in the aIPS, the ventral premotor cortex (a possible homologue of monkey area F5) and the inferior frontal gyrus during grasping. In general, human studies confer the impression of a visual grasping network similar to the monkey AIP – F5 – M1 circuit. However, the delineation is not as clear, and further areas like the prefrontal cortex, the primary somatosensory cortex and the superior parietal cortex appear to be involved as well (Castiello, 2005; Davare, Kraskov, Rothwell, & Lemon, 2011).

In summary, integration of visually acquired target object information into grasp control is procured by a neural network of specialized areas in the parietal and frontal cortex. Electrophysiological studies of non-human primates could identify the areas AIP and F5 as key regions involved, with AIP focusing on the extraction of grasp relevant information, and F5 selecting the appropriate grasp

motor command, and initiating the grasp movement via connections to the primary motor cortex, brain stem, and even spinal cord. While methodological limitations make it impossible to study the human neural grasping networks in similar detail, compelling evidence for a similar organization has been collected in lesion and imaging studies, with the areas aIPS and PMv being possible homologues of monkey areas AIP and F5.

3.1.5 Linking perception and action: the impact object recognition on human grasping

The influence of familiar object size on reach to grasp kinematics towards differently sized spheres has been investigated in a sphere grasping experiment by Marotta and Goodale (2001): the absence of familiar size cues indeed led to an increase in the number of on-line movement corrections characterized by additional movement velocity and aperture peaks and velocity and aperture plateaus per trial. However this increase could only be observed in monocular viewing conditions. Under binocular viewing conditions no significant differences in movement aperture and velocity profiles could be detected between the varying sphere size and the familiar sphere size arrays. The authors attributed this finding to the dominant role of binocular cues, i.e. direct physical size and distance information under binocular viewing conditions. Thus familiar size cues, presumably processed by the ventral occipitotemporal stream, are employed in reach to grasp planning only when binocular vision is denied. However the authors acknowledged that the spheres used in the experiment had never been encountered by the participants prior to the experiment; and the employment of more familiar everyday objects might yield further insight into the use of explicit object knowledge in reaching and grasping. Haffenden and Goodale (2002) procured another investigation by linking square block sizes to colour cues: red = large; yellow = small and vice versa. When the blocks were presented in the same location learned perceptual information had a large influence, whereas when presented in different locations actual physical object properties were primarily drawn upon during grasping. The issue of learned perceptual information was further inquired upon in a behavioral study

(McIntosh & Lashley, 2008) where the participants had to perform a reach to grasp task towards matchboxes of brands widely familiar in the investigated population. Contrary to Marotta and Goodale (2002), McIntosh and Lashley (2008) found a significant influence of familiar size in the binocular as well as the monocular conditions. They argue that this finding can be explained by the meaningful character of the employed objects in contrast to the abstract spheres. The influence of familiar size on the reach to grasp movement cannot be explained without a top down influence of stored object knowledge. Thus the ventral occipitotemporal pathway might be continuously contributing information to the brain areas of action control. It could be argued, that the results of this study are mediated by short term learning effects rather than established object knowledge. In another experiment by Borchers, Christensen, Ziegler, and Himmelbach (2011), a significant influence of short term learning could not be found in binocular viewing conditions. A further investigation of reach to grasp movements towards meaningful everyday objects and cuboids of matched physical dimensions, and even cuboids of matched surface colour as well as shape revealed a significant impact of object familiarity on the mean grip aperture (Borchers & Himmelbach, 2012). This provides additional arguments for the importance of prior object knowledge for the implementation of motor parameters for grasping.

Object familiarity thus has the greatest impact on reach to grasp movement kinematics in monocular viewing experimental setups. Monocular viewing conditions provide a reduced number of visual spatial cues and therefore the visuomotor grasping network has to make greater use of other visual cues, including object familiarity. However, even in binocular reach to grasp paradigms, an influence of object familiarity is evident, if the participants are well accustomed with the objects. In an environment where humans have to deal with a high level of redundancy of grasp targets in daily life, it seems very likely that prior object knowledge is indeed employed to facilitate grasp motor planning.

3.2 Magnetic resonance as a tool for functional imaging of the human brain

3.2.1 Magnetic resonance imaging

Magnetic resonance imaging (MRI) is an investigation technique based on the behaviour of atoms in a strong magnetic field. The atom of choice is typically hydrogen, as it is abundantly present in human tissue. In a strong static magnetic field B_0, the spin axes of hydrogen atoms align with the axis of the magnetic field. As they do, the spin axes obtain an alignment either parallel or antiparallel to B_0, with a very small excess of only 0.0001% of atoms aligning in the parallel direction. However, taken the vast number of atoms in human parenchyma, this excess is sufficient to create a macroscopic magnetization vector M. M is parallel to B_0 at this point; it is being labelled M_0 and cannot be measured directly. Therefore it has to be diverged from its equilibrium state. This is achieved by applying a high frequency pulse (HF-Pulse) transverse to the static magnetic field B_0. By choosing a pulse frequency close to the proton rotation frequency (i.e. 127.8 MHz in a 3T field), a resonance effect is fulfilled and M starts do deviate from B_0. With the employed flip angle of 90° M is being brought into the plain transversal to M_0. As soon as the HF-Pulse is over, M starts to move back to its equilibrium state, relaxing both in the longitudinal and the transversal axis. By choosing an appropriate repetition time TR and echo time TE, the captured signal intensities can rely mainly on the longitudinal relaxation speed (i.e. T1 time), or on the transversal relaxation speed (i.e. T2 time). T1-weighted images have a short TR and a short TE; T2-weighted images have a long TR and a long TE. If dephasing caused by magnetic field inhomogeneities and susceptibility effects are being accounted for additionally to the T2 time, the resulted contrast is being called T2*-weighting, which has proven appropriate for functional brain imaging (Ogawa et al., 1993). For more details on the MR physics and applications at higher field strengths (3T) see Schick (2005).

3.2.2 Blood oxygenation level dependent functional MRI

Since the first demonstration (Ogawa, Lee, Kay, & Tank, 1990), MRI has become an invaluable tool in neuroscience, due to the capability to non-invasively provide an inference of neuronal activity in the brain, with a good spatial and temporal resolution. But how does MRI measure neuronal activity? As described above, magnetic field inhomogeneities influence the T2* time: larger inhomogeneities lead to a shorter T2* time and thus faster signal decay. If the measuring time point remains unchanged (TE constant), greater magnetic field inhomogeneities lead to a weaker signal in T2*-weighted images. But what physiological state changes the level of such inhomogeneities within a volume of tissue? The answer is blood oxygenation: oxyhaemoglobin is weakly diamagnetic and has very little effect on the magnetic field, while deoxyhaemoglobin is paramagnetic and induces dephasing. This means that brain voxels (volumetric elements) with a lower concentration of deoxygenated haemoglobin show a higher signal in relation to voxels with a lower deoxyhaemoglobin concentration. The typical signal change in a brain voxel following neural activity, and the corresponding physiological haemodynamic reaction in that area is called a BOLD (blood oxygenation level dependent) response. The canonical model of a BOLD response consists of 3 phases: an initial lowering of the signal due to immediate oxygen consumption, a larger signal increase caused by the following excessive oxygen supply, and a gradual decrease below the baseline level. Following neural activity in a region, increased metabolic demand leads to increased oxygen exhaustion and thus increased deoxyhaemoglobin concentration. After a delay of about 2s, capillary dilation increases the local blood flow (functional hyperaemia), overcompensating for neural oxygen extraction. Mechanisms responsible for this haemodynamic response are possibly triggered by products of astrocyte metabolism (lactate) and neuronal activity (nitric oxide), or may represent a vascular reaction to blood deoxygenation. For review see Heeger and Ress (2002).

The relation between stimulus intensity and fMRI BOLD response has been investigated by (Boynton, Engel, Glover, & Heeger, 1996). It has been shown, that the BOLD signal generally fulfils the basic properties of a linear system: scaling (proportionality of the signal to the magnitude of the input stimulus) and superposition (signal output after multiple consecutive stimuli is equal to the sum of the outputs measured after individually presented stimuli). This linearity was already presumed in earlier Studies (P. A. Bandettini, Jesmanowicz, Wong, & Hyde, 1993). Based on this insight a linear transform model for BOLD signals has been developed. On the one hand it allowed for relating a recorded output from a volume element (voxel) to the underlying stimulus. On the other hand, we can apply the opposite approach, and search the recorded brain volume for voxels that show a response similar to the one we calculated based on a known stimulus. By statistically testing for this similarity we can create statistical parametric maps (SPMs) of the brain (Friston et al., 1995).

3.2.3 Echo planar imaging

Echo planar imaging (EPI) is a magnetic resonance imaging technique capable of recording an image in as little as <100ms. This is achieved by oscillation of the frequency-encoding gradient from positive to negative amplitude after the HF-Pulse has been applied. Such a process allows for image reconstruction after one single excitation pulse, thus effectively eliminating motion artifacts within the particular acquired slice. EPI is therefore perfectly suited for functional imaging of dynamic tissues like the human brain. Please note that only one slice is recorded at a time. By combining the consecutively acquired slices of the brain we record a volume; in our case 36 adjoining 3mm slices were recorded within a repetition time TR of 2.47 seconds. For EPI review see Poustchi-Amin, Mirowitz, Brown, McKinstry, and Li (2001).

3.2.4 Blocked and event related fMRI experimental design paradigms

In principle there are 2 ways of conducting an fMRI experiment: A ‘block design’ using stimuli that have close temporal proximity or an ‘event-related design’ where each stimuli are separated by a bigger interstimulus interval.

Blocked designs exploit the superposition principle of linear systems, thus achieving a higher measured signal within the brain regions responding to a particular stimulus, by presenting stimuli of a similar type continuously for a specific time period (block). The different block categories are presented alternatingly. Blocked designs have a higher overall detection rate, and were therefore adopted for our visual presentation experiment.

Event-related designs rely on longer interstimulus intervals, with 12s and beyond recommended by Bandettini and Cox (2000). Therefore a smaller number of trials can be conducted within the same time, reducing overall signal variance, and therefore detection power. However, event-related paradigms allow for better time-course estimation and are more flexible during data analysis. Most importantly, they greatly reduce susceptibility to motion related artifacts: caused either by direct head movement during task execution, or through motion-induced changes in the magnetic field (Birn, Bandettini, Cox, & Shaker, 1999). This was the main reason for us to employ an event-related design in the grasping experiment. We also planned for the grasping experiment to take longer, and ran more grasping sessions than visual presentation sessions in order to partially compensate for the inferior detection.

3.2.5 Difficulties of motor studies in fMRI

FMRI has established itself as a dominant technique for studying brain activity in humans. Over the last two decades technological advancement and data processing techniques have contributed to the improved sensitivity and reliability of fMRI data analysis. Considerable effort has been put into strategies accounting for movement related artifacts. 30-90% of the fMRI signal can be attributed to movement, and with appropriate measures most of this artificial component can be removed (Friston, Williams, Howard, Frackowiak, & Turner, 1996; Grootoonk et al., 2000). More complex solutions have been developed to deal with large amounts of movement related artifacts in investigations involving clinical conditions, like fragile X syndrome, attention deficit/hyperactivity disorder, and pediatric patients (Mazaika et al., 2009). However, once participant movement itself becomes the target of an fMRI investigation, these

measures do not suffice. A major issue is the big variance in exhibited participant behavior. The majority of fMRI motor studies do not involve systematic control of participant action. Only recently investigators have begun to record exhibited participant behavior in fMRI studies (Cavina-Pratesi, Goodale, & Culham, 2007; Verhagen, Dijkerman, Grol, & Toni, 2008), and no uniform strategy of implementing behavioral parameters within the fMRI data analysis pipeline exists as yet. We have therefore put a lot of emphasis on capturing and analyzing participant behavior using an MR compatible video recording system. We also procured a systematic examination of possible implementations within the functional brain data analysis in order to determine a strategy best suited to our experimental setup.

3.3 Aims of this study

The aim of this study was to determine anatomical correlates of visuomotor integration during reach to grasp action planning for meaningful objects in humans. We challenge the statement, that dorsal stream regions only deal with physical properties of the grasped object such as its size and position in relation to the grasping limb (M. A. Goodale & Milner, 1992). We hypothesised that prior object knowledge plays a major role in grasp action planning of frequently used everyday objects, and is being processed in grasp related areas of the dorsal stream, in particular the anterior intraparietal sulcus and the ventral premotor cortex.

Additionally, we pioneered methodological approaches for the appropriate utilization of kinematic parameters in functional magnetic resonance imaging. For this purpose we established an array of graspable real world objects we expected to be well known to our participants, and acquired the functional brain imaging data during the viewing and grasping of these objects. Parallel to functional brain imaging, basic kinematic parameters of grasping were recorded. This provided us with a wide set of data to best link the exhibited neural and behavioural responses.

4. Materials and Methods

4.1 Reach to grasp movement fMRI study experimental design

4.1.1 Participant recruitment

29 healthy individuals (19 female, Age 25.8 ± 2.7 years) volunteered for the experiment, of which 27 completed the full experiment (18 Female; 9 Male; Age 25.9 ± 2.8 years) and as such were included in the analysis. They were recruited from the community of Tübingen (Baden-Württemberg, Germany) and gave their informed consent in accordance to the University of Tübingen's Medical Faculty's Ethics Board. All measurements were performed in accordance with the ethical standards established by the 1964 declaration of Helsinki. All participants were right handed according to self-report, and had normal or corrected to normal visual acuity.

4.1.2 Experimental stimulus categories and presentation properties

The stimuli used within this experiment were real objects that could easily be designated to one of two categories: four well known familiar objects (FAM); an eraser; a matchbox; a highlight marker pen and a packet of paper tissues. These objects are commonly used during routine daily activities and are ones that our participants knew well (Figure 1). Secondly, four simple geometric objects (GEO): unicolour wooden blocks, each with a dimension that matched a respective familiar object. These items were considered to be association free objects, i.e. ones that are not primarily linked to a task and most likely have not been previously grasped before the experiment.

Of these objects we categorized the eraser, the matchbox and the matching wooden blocks into the 'small' subcategory, while the highlight marker pen, the tissue paper packet and the correspondingly sized wooden blocks were considered 'big'. The objects were attached via Velcro to a plastic presentation

plate. The plate itself had 2 Velcro loop stripes: a thin one at the top half and a thick one at the bottom half. The objects can be easily attached to either one, however were always presented on the top. The plates match a slot in the presentation platform and can be exchanged without difficulty from outside the scanner.

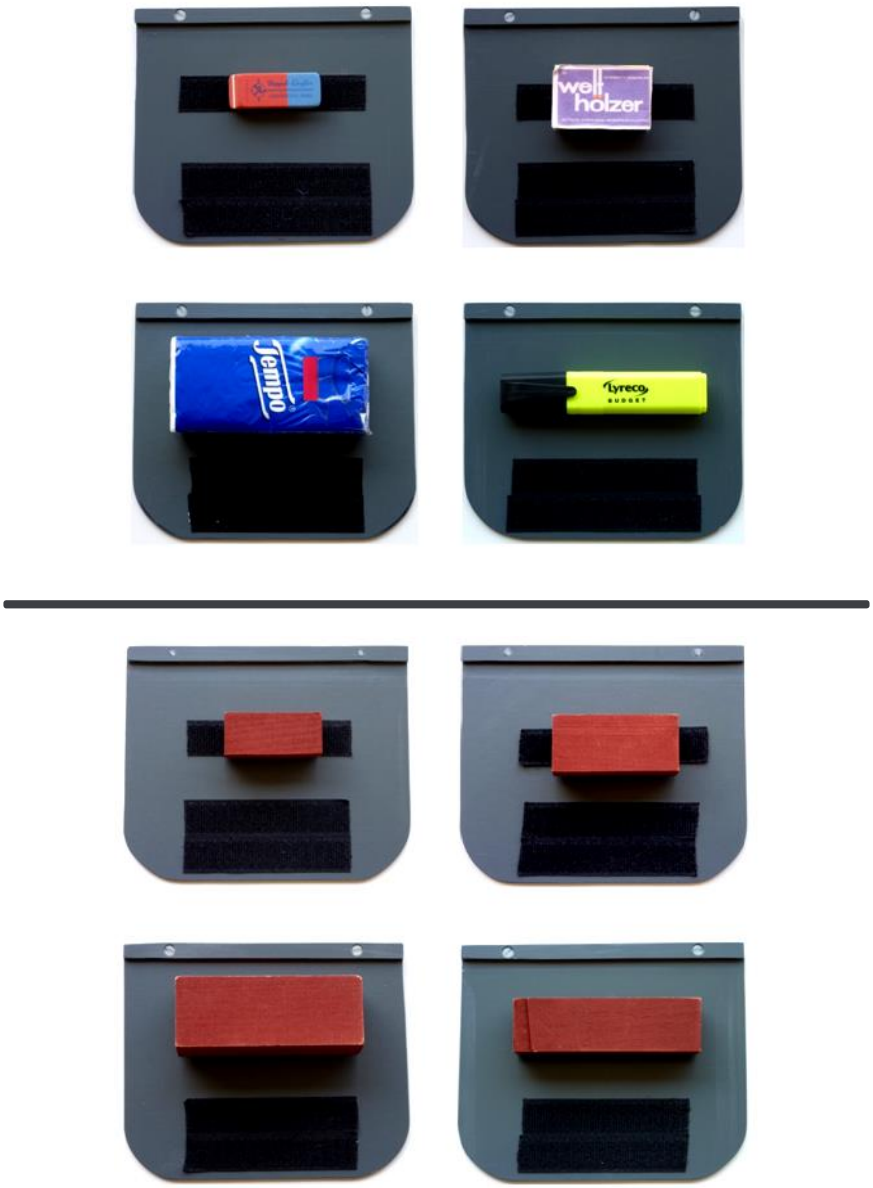

Figure 1:

Familiar objects (FAM) are shown in the upper panel and geometric objects (GEO) in the lower panel. Each displayed attached to a retractable plastic plate used in the experiment. The geometric objects were custom made to match the dimensions of their familiar counterparts.

4.1.3 Experimental setup

Figure 2 presents a participant positioned in the experimental setup. Participants were positioned within the MRI in a comfortable position with their head tilted at an angle of ~25° to allow a clear and direct visibility of the objects. Ear protection and feedback means (including an emergency alarm ball) were provided. Additional head support was provided using several foam cushions to minimise head movements. The participants' right elbow was firmly strapped to their chest in order to restrict the amount of motion being transferred to neck and head during grasping. A conveniently held plastic box with a single button on the side was attached to the individuals' chest, and served as a defined resting place for the participants' right hand outside of trial execution periods. The button was held either with the thumb or the middle finger of the right hand according to the participant's preference and was only to be pressed during defined periods of the visual presentation trials. The left hand was resting upon the emergency alarm ball somewhat below the left anterior superior iliac spine, and should not be moved during the course of the experiment.

Above the participants' pelvis we mounted the presentation table. It consisted of a platform skewed at a 45° angle toward the participant's head, and therein a slotted retractable plate, upon which the objects could be attached to via a hook and loop fastener. The table's position was individually adjusted to achieve the best object visibility possible, while allowing for an unconstrained reach to grasp movement and maintaining overall postural comfort. The presentation light source (white) was attached above the head coil facing the presentation table; the fixation/instruction light (red/green respectively) was placed approximately 10cm above the experimental table facing the participant. The lights consisted of numerous optic fibre cables connected to a programmable LED situated outside the scanner room.

Experimental timing including presentation, fixation and instruction LED control was determined by a custom-made script created with Matlab (Math Works).

Object randomization was performed manually by the person exchanging the object plates in the scanner room.

For real-time behavioural monitoring and recording we used 3 MRI compatible cameras. 2 of them were small “12M” MR cameras (MRC Systems, Heidelberg, Germany) capturing hand movement, installed upon adjustable shafts at the head end; these cameras were therefore moved within the scanner bore during participant positioning. The third camera (SensoMotoric Instruments, Teltow, Germany), was positioned behind the scanner, focusing an eye mirror set up above the head coil.

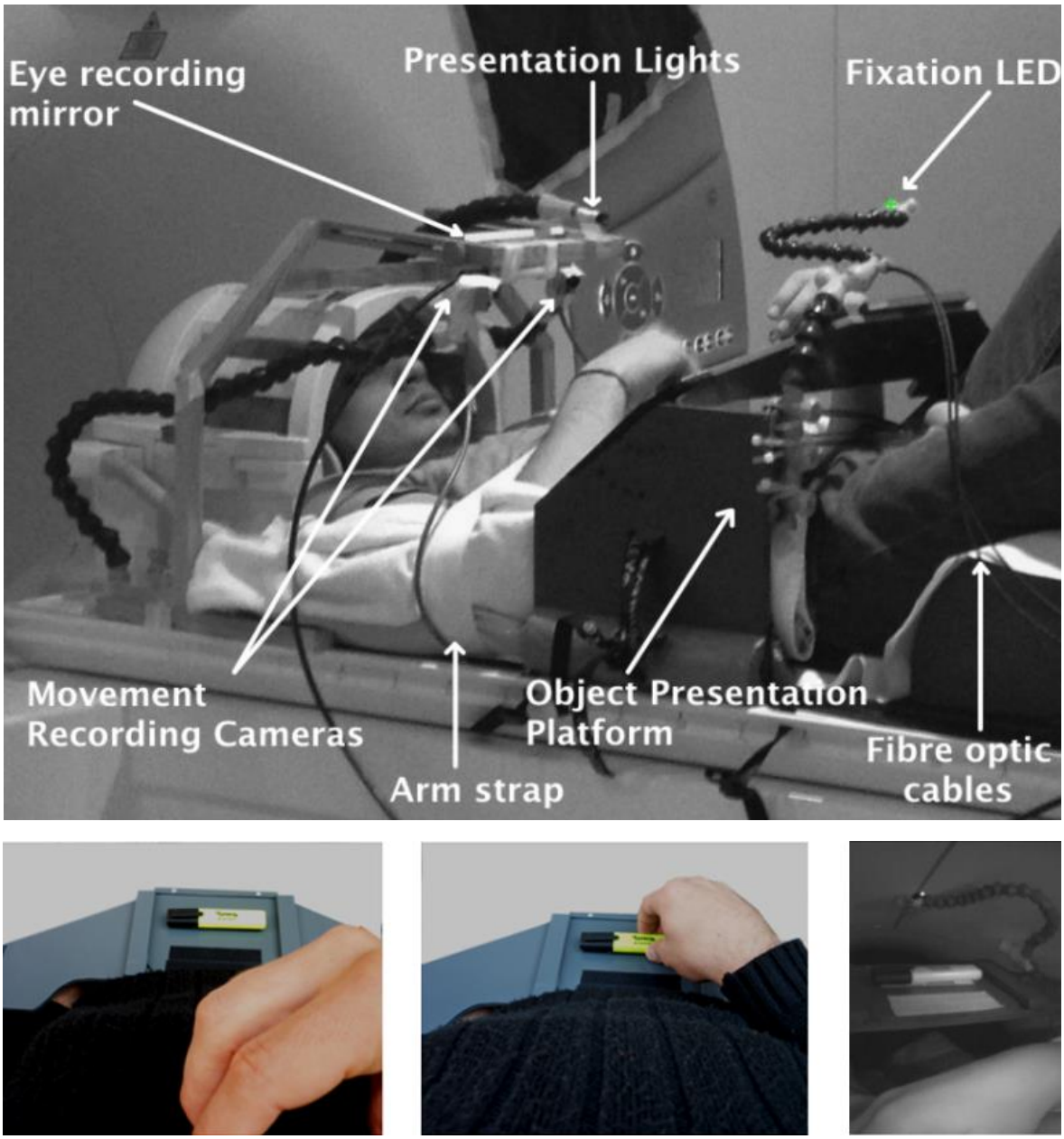

Figure 2:

Upper image: experimental equipment included a custom made object presentation platform, fixation and presentation lights lit through an external LED via fibre optics and an arm strap reducing transmission of arm movement to the head. Monitoring equipment consisted of 2 MR compatible video cameras designated specifically for hand movement recording and a separate mirror-camera system recording eye movement.

Lower left and middle images: participants reached from a start position above their sternum to the presented objects, lifted them up, placed them on the lower part of the platform, and returned to the starting position; viewed from the participant‘s point of view.

Lower right image: A perspective of one camera within the scanner. Please note the whole experiment was performed in complete darkness, except for the short object presentation time of 250ms.

4.1.4. Experimental procedure

The subject matter of our investigation, i.e. visually guided reach-to-grasp movements is a complex process. To best accommodate the challenge of attaining the most valid result possible, we decided to conduct two distinct experiments. The first experiment (‘grasping’) consists of the actual reach-to-grasp tasks we were interested in. The second experiment (‘visual presentation’) was a control experiment. We conducted it in order to test whether potential differences between object categories observed during the grasping trials can also be caused by attentive viewing of the objects. Grasping and visual presentation sessions were conducted alternately within each participant’s trial run. During both experiments lighting and experimental timing was controlled by a custom made MATLAB® (The MathWorks, Inc) script. A detailed explanation of both trial types is provided below.

It is important to mention that except for the brief object illumination periods the participants stayed in complete darkness. This served the purpose of ruling out activations caused by non-experimental visual stimuli (Culham et al., 2003) and avoiding a visual stimulation by the executed arm movements. MRI scanner control lights and scanner room windows were covered by opaque black plastic foils. To minimize the participants’ dark adaptation scanner room lights, additionally to the multiple periods of object presentation, were turned on between sessions. To minimize avoidable eye movement, participants were instructed to look at the small fixation light just above the presentation platform whenever no objects were presented for grasping or attentive viewing.

4.1.4.1 Grasping experiment design

The purpose of this experiment was to record cerebral BOLD responses while the participants grasped objects of the familiar and geometric category. An event-related design was chosen based on previously reported observations to minimize movement artifacts (Birn et al., 1999; Culham et al., 2003).

Preceding the experiment the participants were individually trained for approx. 30 minutes in an improvised setup reflecting the one in the scanner. They were asked to perform the grasping task under daylight level luminance with their eyes open in the first half of the training. In the second half they had their eyes closed and opened them only for a short duration just before performing the grasping task, thus mimicking the experimental procedure in the scanner. A tactile stimulus (a light tip on the participants shoulder) was used as a start signal. Arising questions were straightened out, and fluid task execution was verified by the instructor.

The participants were situated in the setup as described above. They were instructed to perform the task as soon as the object was illuminated by the light source. The illumination continued only for a brief period of 250ms, i.e. shorter than the expexted minimal response time. Consequently the task would be carried out in darkness (open loop excecution without visual feedback). The task was for the participants to reach out to the presented object, grasp it, lift it from the upper part of the plate, place it on lower part of the plate and return their hand to the starting position (Figure 2). The entire movement was to be performed with the right hand, as fluidly and naturally as possible. Then the plate was replaced by an experimenter by one with a different target object. 18-20s after the light onset the next trial was started by the next light onset. Objects were presented in random order (Figure 3a). 32 grasping trials were conducted during a grasping session, with most participants completing 5 sessions (2 participants completed 4 sessions, 3 participants completed 3 sessions).

4.1.4.2 Visual presentation experiment layout

We conducted a complementary control experiment in order to identify activation patterns originating from mere attentive viewing of the familiar and geometric object categories. A block design was chosen to maximize the HRF response during the relatively simple task as opposed to grasping.

The participants were lying in the previously depicted setup in darkness, exactly as in the grasping experiment. They were instructed to attentively

observe the objects, which were presented in blocks of 5 of the same category (either FAM or GEO). Meaning that during each presentation block every individual object of the respective category was shown at least once with one object presentation repeated. Presentation occurred through illumination of each object using the LED based light source (250ms), with 4.75s within-block intervals between objects, and 20s intervals between blocks (Figure 3b).

Additionally, to ensure that attention was being paid to the presented objects, an odd-one-out task was given. Several times per session an oddball object that belonged to neither category was presented instead of one of the 5 objects of a block. During the following 20s interblock interval, a flashing of the green instruction LED asked the question: “Did you see the oddball object in the previous block?”. The participant answered via a button press: “yes” by pressing the button at his right hand's resting place, and “no” by not pressing it. Question timing was specified by a randomized sequence to compensate for fluctuations in the baseline BOLD response.

The presentation of objects and object category was randomized and counterbalanced across sessions, such that within a visual presentation condition both FAM and GEO were presented an equal number of times per participant. 10 presentation blocks and 10 interblock intervals made up a visual presentation session, with the majority of participants completing 4 sessions (3 carried out 3).

(a)

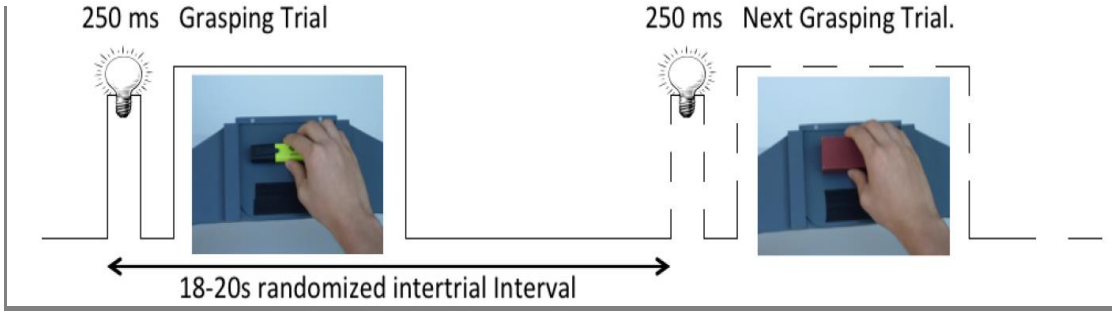

(b)

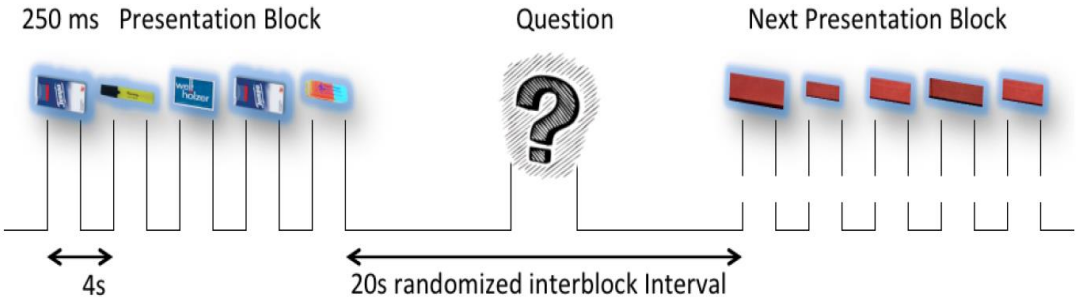

Figure 3:

(a): Procedure schematic of a grasping session. Brief object illumination serves as a start signal for grasp execution. After each trial the participant returns his hand to the original position waiting for the consecutive start signal.

(b): Procedure schematic of a visual presentation session. Objects of the same category were presented in blocks of 5 via 250ms light flashes each. Attention maintenance was established by an odd-one-out task: several times per session an oddball object would be interspersed. In between blocks a blinking of the green instruction light would prompt the participants to press a button if they perceived the oddball during the preceding block.

4.2 Functional and anatomical MRI image acquisition

4.2.1 Scanner model and functional volumes imaging specifications

A 3T MRI scanner (Siemens Magnetom Trio, Erlangen, Germany) was employed for our experiment. A standard 12 channel head coil was chosen over the fitted 16 and 32 channel head coils to allow space for the tilted head position as required by our setup. The scanner runs consisted of 182 T2*-weighted EPI Volumes for each of the visual presentation experiment sessions and 260 volumes for each grasping session (slice thickness = 3mm; 36 slices interleaved acquisition; in-plain resolution 3mm × 3mm; TR = 2.47s; TE = 33ms; flip angle = 90°). The slices were aligned approximately parallel to the anterior to posterior commissure line; the full volume covered the cerebrum, mesencephalon, pons and the upper 2/3 of the cerebellum.

4.2.2 Anatomical volumes imaging specifications

For each participant a high resolution anatomical image was attained with a T1-weighted MP-RAGE sequence (slice thickness = 1 mm; 176 sagittal slices; in-plain resolution 1mm × 1mm; TR = 2.3s; TE = 2.92ms; flip angle = 8°). The resulting image covered the participants' complete head and neck above C5.

4.3 Hand movement and eye movement recording

4.3.1 Eye movement video recording

Eye movements were captured throughout the entire fMRI measurement using a long-range eye tracking system (SMI SensoMotoric Instruments, Teltow, Germany). It was positioned behind the scanner bore and adjusted to face a mirror above the participants' eyes. Data were sampled at 30Hz and digitized for offline analysis. As the participant's head position deviated from standard positions due to the experimental setup, automated saccade detection software did not work properly, and was therefore not employed. The images from the eye camera were viewed online; if major fixations deficits could be detected, the experiment was interrupted, the participant reminded of the instructions and the respective scanner run repeated. Later on, the recordings were controlled manually for undesirable eye movements, i.e. non task or fixation related, to be taken into account during data analysis.

4.3.2 Hand movement video recording

Hand movement was recorded during every scanner run using 2 miniature MR-compatible infrared cameras (MRC Systems, Heidelberg, Germany). They were positioned at both sides of the head coil, together covering both hands and the entire reach to grasp movement during grasping trials if possible. Data were sampled at 30Hz and digitized for offline analysis. As with the eye movement recordings, hand camera images were viewed online. If the participants did not carry out the instructions correctly, the session was stopped and the participants were instructed again, and then the session was restarted

The videos were subsequently viewed offline and analysed for all visible components of the reach-to-grasp movement: response time, response to reach, reach to lift, lift to placement, placement to return onset, and return onset to finish durations. Error trials were identified, either based on obvious deviations from the instructed reach-to-grasp procedure (object drop, no action performed etc.), or if an individual response time was outside of the respective

patient's mean ± 2.5 SD. In total, only 132 of 3520 single trials were labelled as error trials across all participants (i.e. 3.75%).

During the visual presentation sessions, hand movement recordings were used to verify that the participants only moved to press the button as instructed.

4.4 FMRI data analysis pipelines

4.4.1 FMRI data preprocessing

For the analysis and preprocessing of the functional images attained in our experiment we used the statistical parametric mapping software SPM8 (Wellcome Trust Centre for Neuroimaging, London, UK) implemented into Matlab R2011b (MathWorks Inc., Natick, USA).

Data preprocessing was as follows: The first 5 volumes of each scanner run were removed to make sure that the MRI signal reached its steady state. The remaining volumes were spatially realigned to the first image in order to correct for the participant's head movement. Subsequently we applied a slice timing correction to the volumes (Sladky et al., 2011). The anatomical T1 weighted volume was then coregistered to the mean functional EPI image. Afterwards both the anatomical and the functional images were grossly manually aligned to the T1 MNI Template (distributed with SPM8) and then coregistered to it. Then the anatomical image was segmented and spatially normalized to the T1 MNI Template with the unified segmentation and normalization procedure. The resulting transformation parameters were applied to the EPI volumes as well. Finally the functional images were smoothed with an isotropic FWHM (full width at half maximum) 9mm Gaussian kernel.

White matter and residual (exterior of the skull) compartments were extracted using the ‘New Segmentation Toolbox’. Signal changes in these regions are most likely artefact related and were therefore filtered in an additional covariate during the fixed effects analysis. To extract the signal courses in these compartments, white matter and residual compartment masks were thresholded with a probability value of 0.99, and then read out using the MarsBar SPM toolbox (Brett, Anton, Valabregue, & Poline, 2002).

4.4.2 Standard approach without kinematics integration

While fMRI data analysis pipelines can vary considerably between studies, a particular set of measures to deal with motion-related artifacts is used in most current investigations (Friston et al., 1996; Grootoonk et al., 2000). This approach, further referred to as the 'standard approach', encompasses the following range of strategies. Extreme outliers and unsuccessful trials have been identified (error trials, see section 4.3), and subsequently excluded into a separate category for the fixed effects analysis. Therein, realignment parameters as well as white matter and residual compartment time courses were implemented as covariates. Undesired eye movement, i.e. horizontal saccades during grasping and attentive viewing sessions have also been identified, and modeled as two separate regressors. However, no steps were taken to incorporate the actual movement kinematics into the analysis.

4.4.2.1 Standard approach fixed effects analysis

Within the first level fixed effects analysis a high-pass filter with a cut-off period of 128s was implemented to remove low-frequency drifts. An autoregressor was applied to correct for temporal autocorrelation within the data. To optimally incorporate the physiological diversity of the haemodynamic response in different parts of the brain, the experimental conditions were modelled by a boxcar function convolved with the canonical HRF including temporal and dispersion derivatives.

A GLM design matrix with one parameter per condition of interest was designed: Visual Familiar Big; Visual Familiar Small; Visual Geometric Big; Visual Geometric Small; Visual Bad Trials; Visual Oddball; Saccade during Presentation Block; Saccade outside Presentation Block; Grasp Familiar Big; Grasp Familiar Small; Grasp Geometric Big; Grasp Geometric Small; Grasp Bad; Saccade during Grasp Event; Saccade outside Grasp Event. For the Visual Presentation trials, object presentation times and durations (250ms) were entered into the design matrix. For the Grasping trials object presentation times were logged as onset times and individual response times as durations.

Covariates included in the first level analysis were realignment parameters determined during the preprocessing (3 rigid body translations and 3 rotations: pitch, roll and yaw) to effectively deal with residual movement related artefacts. Additionally, the time courses obtained from the white matter and residual compartments were added as additional covariates, that reliably deweight activations unrelated to primary substrates of neural activity, i.e. grey matter (Verhagen, 2012).

After the estimation of the general linear model (GLM), linear contrasts were applied to the parameter estimates of the events of interest, in order to test the effects of our experimental conditions.

4.4.2.2 Standard approach random effects analysis

The random effects analysis was conducted using the contrast images obtained from the first level GLM. Familiar and geometric categories were compared with a voxelwise paired t-test among visual and among grasping trials separately. Significant findings are reported in the Montreal Neurological Institute (MNI) stereotactic reference space. Interpretation was based on consistent neuroanatomical landmarks, probabilistic cytoarchitectonic maps (Eickhoff et al., 2005) and preceding research on visuomotor grasping networks (see Introduction).

4.4.3 Balancing the included trials with regard to a kinematic parameter approach

The general procedure was very similar to the standard approach reported above. The difference mainly consisted in the particular trials included in each category. In order to minimize the differences between familiar and geometric conditions with respect to a chosen kinematic parameter, additional trials were assigned to the error trial category. Trials selected to be assigned to the error trial category were the ones with more extreme kinematic values, both the unusually short and unusually long ones. Due to the complex nature of the distribution of these parameters, balancing could only be achieved for one parameter at a time. Therefore, response time

(RT), and complete movement time (MT, response to finish duration) have been chosen as exemplary parameters for this analysis. These were also the parameters that can be measured without continuous video recording, for example using a button based setup by workgroups without access to MR-compatible video recording equipment.

As an example we shall take a look at RT balancing in a hypothetic set of 10 trials (5 familiar, 5 geometric), with the response times of 1s, 2s, 2s, 3s and 3s (mean = 2.2s) during grasping familiar objects, and 2s, 2s, 3s, 3s, and 4s (mean = 2.8s) during grasping geometric objects. Here, the procedure would involve discarding the 1s RT familiar, and the 4s geometric trial, resulting in two 4 trial sets with equal means of 2.5s. Note however, that this is an ideal example, and in practice both untypically long and untypically short kinematic values were present in both categories. The reasoning behind the balancing procedure is that the remaining differences in the consecutive statistical analysis are driven by the object category, and not the RT difference.

4.4.3.1 Balancing the included trials approach fixed effects analysis

Within the first level fixed effects analysis a high-pass filter with a cut-off period of 128s was implemented to remove low-frequency drifts. An SPM8 autoregressive process was applied to correct for temporal autocorrelation within the data. The experimental conditions were modelled by a boxcar function convolved to the canonical HRF including temporal and dispersion derivatives.

A matrix with one regressor per condition of interest was designed: Visual Familiar Big; Visual Familiar Small; Visual Geometric Big; Visual Geometric Small; Visual Bad Trials; Visual Oddball; Saccade during Presentation Block; Saccade outside Presentation Block; Grasp Familiar Big; Grasp Familiar Small; Grasp Geometric Big; Grasp Geometric Small; Grasp Bad; Saccade during Grasp Event; Saccade outside Grasp Event. For the Visual Presentation trials,

object presentation times and durations (250ms) were entered into the design matrix. For the Grasping trials object presentation times were logged as onset times and individual response times as durations.

Covariates included into the first level analysis were realignment parameters determined during the preprocessing (3 rigid body translations and 3 rotations: pitch, roll and yaw) to effectively deal with residual movement related artefacts. Additionally, the time courses obtained from the white matter and residual compartments acted as another covariate. After the estimation of the general linear model (GLM), linear contrasts were applied to the parameter estimates of the events of interest.

4.4.3.2 Balancing the included trials approach random effects analysis

The random effects analysis was conducted using the contrast images obtained from the first level GLM. Familiar and geometric categories were compared with a voxelwise paired t-test among visual and among grasping trials separately. Significant findings are reported in the Montreal Neurological Institute (MNI) stereotactic reference space.

4.4.4 Reach to grasp kinematics as covariates of no interest approach

In contrast to strategies presented so far, this approach operates on the random effects analysis level. Implementing the kinematic parameters at this step of the analysis can be done by using them as covariates of no interest. This course is very efficient and does not require discarding data, as in the Balancing the included trials with regard to a kinematic parameter approach, see section 4.4.3. Several covariate combinations described below have been tested. The fixed effects analysis on the other hand corresponds to the standard approach, see section 4.4.2.

4.4.4.1 Reach to grasp kinematics as covariates fixed effects analysis

Within the first level fixed effects analysis a high-pass filter with a cut-off period of 128s was implemented to remove low-frequency drifts. An SPM8 autoregressive process was applied to correct for temporal autocorrelation within the data. The experimental conditions were modelled by a boxcar function convolved to the canonical HRF including temporal and dispersion derivatives.

A matrix with one parameter per condition of interest was designed: Visual Familiar Big; Visual Familiar Small; Visual Geometric Big; Visual Geometric Small; Visual Bad Trials; Visual Oddball; Saccade during Presentation Block; Saccade outside Presentation Block; Grasp Familiar Big; Grasp Familiar Small; Grasp Geometric Big; Grasp Geometric Small; Grasp Bad; Saccade during Grasp Event; Saccade outside Grasp Event. For the Visual Presentation trials, object presentation times and durations (250ms) were entered into the design matrix. For the Grasping trials object presentation times were logged as onset times and individual response times as durations.

Covariates included into the first level analysis were realignment parameters determined during the preprocessing (3 rigid body translations and 3 rotations: pitch, roll and yaw) to effectively deal with residual movement related artefacts. Additionally, the time courses obtained from the white matter and residual compartments acted as another covariate. After the estimation of the general linear model (GLM), linear contrasts were applied to the parameter estimates of the events of interest.

4.4.4.2 Reach to grasp kinematics as covariates random effects analysis

The random effects analysis was conducted using the contrast images obtained from the first level GLM. At this stage we incorporated the individual mean values for the components of the reach to grasp movement, observed during the offline hand movement recording inspection, as additional covariates for the group analysis to best accommodate the effect of the experimental conditions on the kinematic parameters of the movement (see section 5.1). Investigated covariate combinations were: response time only, complete movement time only (as mentioned above, these parameters could also be measured without continuous video recording); as well as all 6 movement components in a block of 6 independent covariates: this was the most detailed information that our video analysis provided, and should therefore be the most precise one. Familiar and geometric categories were compared with a voxelwise paired t-test among visual and among grasping trials separately. Significant findings are reported in the Montreal Neurological Institute (MNI) stereotactic reference space.

4.4.5 Region of interest extraction

Based on our evaluation of implementation strategies of movement kinematics (see section 5.2), including reach to grasp kinematics as covariates into the random effects analysis has proven to be the analysis method of choice for our dataset. At this point we wanted to get a more in-depth comparison. While the statistical maps provided by SPM 8 offer an excellent way to identify brain areas showing significantly different responses for the experimental conditions, they do not allow for a direct investigation of the MRI signal. This is especially crucial when comparing different design paradigms, i.e. blocked design (visual presentation trials) and event-related design (grasping trials). We therefore defined regions of interest (ROIs) by constructing spheres with a 4mm radius around the observed activation peaks, and extracted the respective percent signal changes of each ROI using the MarsBar toolbox (Brett et al., 2002). The resulting values were then compared directly, and, where appropriate, further analysed via a 2-tailed paired T-test.

5. Results

5.1 Effect of object category on reach to grasp kinematics

Essential kinematic data of the participants' reach to grasp movements have been evaluated as described in the Section 4.3. Figure 4 and table 1 show a summary of the means and standard errors of the mean (SEM) of the visible action components. Notably, response time ($P < 0.001$, $t = 4.89$, $df = 26$) and placement to return onset ($P < 0.05$, $t = 2.24$, $df = 26$) time were significantly shorter for familiar objects, while reach to lift ($P < 0.001$, $t= 6.90$, $df = 26$), and lift to placement ($P < .001$, $t = 5.41$, $df = 26$) times were significantly shorter for the geometric objects. These differences, while being subtle, may have had an impact on the functional MRI analysis outcome. We therefore further investigated the issue of integrating kinematic parameters into the GLM functional imaging analysis, and compared the outcome to a standard analysis without the integration of kinematic data.

Using the hand movement video recording we were able not only to identify and exclude incorrectly executed trials, but also determine and compare basic kinematic parameters of the participants' reach to grasp movements. Finding a significant impact of object familiarity on the durations of certain movement parts, the most prominent example being the faster response time for the meaningful objects, confirmed our expectations regarding the importance of prior object knowledge in human grasping. Investigating and taking into account these duration differences within our general linear model was a major consequence of this analysis.

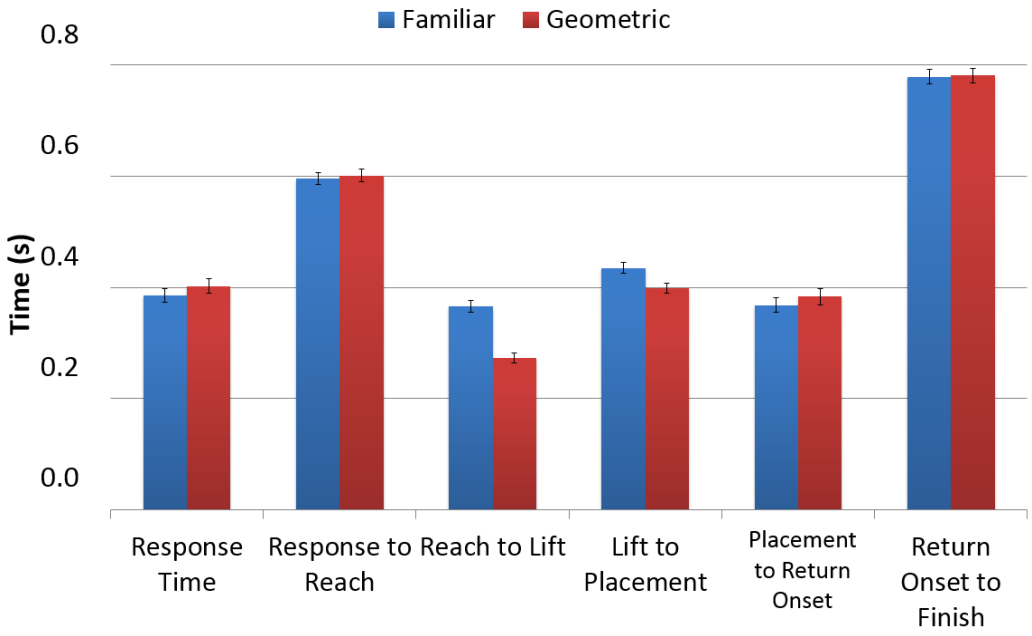

Figure 4:

A bar plot to show the group durations for each movement component (mean ± SEM). Everyday objects (familiar), are shown as blue bars while geometric objects are shown as red bars.

	Fam	Geo	SEM Fam	SEM Geo	p	t
Response Time	390ms	400ms	13ms	13ms	< 0.001	4.89
Time to Object	600ms	600ms	11ms	12ms	0.336	1.37
Object to Lift	370ms	270ms	11ms	9ms	< 0.001	6.90
Lift to Placement	440ms	400ms	9ms	9ms	< 0.001	5.41
Placent to Return Onset	370ms	380ms	13ms	15ms	0.043	2.24
Return Onset to Finish	780ms	780ms	13ms	13ms	0.822	0.47
Total Movement Time	2540ms	2440ms	44ms	44ms	< 0.001	1.98

Table 1:

Mean measured kinematic parameters for all participants during the reach to grasp movements towards familiar objects ‘Fam’ and unicolour geometric blocks ‘Geo’. P and t values were calculated via a 2-tailed paired t-test.

5.2 Evaluation of strategies to incorporate kinematics into the fMRI analysis

To best display the effect of kinematics integration upon the entire analysis process, group results of reaching to and grasping familiar contrasted against reaching to and grasping geometric objects (Grasping (Fam - Geo)) are being consistently presented. Voxelwise analysis results are presented at a significance level of $p < 0.001$ uncorrected, with a cluster threshold corrected for multiple comparisons ($p < 0.05$). This means that each strategy evaluation subsection presents a t-map of significant findings for our main hypothesis (brain areas showing greater signal while reaching to grasp familiar as opposed to geometric objects). The focus lies on the grasping experiment, because no kinematic parameters are recorded, or arm movement tolerated for that matter, during the attentive viewing task.

5.2.1 The standard approach without kinematics integration within the analysis

This analysis represents the currently most common practice in fMRI research, even when movement is involved. The resulting activation pattern should be generally more extended in comparison to approaches integrating kinematics, and will serve as a reference point.

The displayed clusters result from $p = 0.001$ Grasping (Fam - Geo) - t-map ($t = 3.43$), cluster thresholded with $k = 64$, and resulting in a $p < 0.05$ corrected (see figure 5). Prominent activations include the lateral occipital cortex (LOC), ventral premotor cortex (PMv), dorsal premotor cortex (PMd), rostral middle frontal gyrus (rostral MFG), anterior and middle intraparietal sulcus (aIPS, mIPS) on the left hemisphere. Large clusters covering regions of the precentral, postcentral and supramarginal gyrus, anterior cingulate cortex (aCC) and the insular cortex can be observed bilaterally. On the right hemisphere we see well-defined clusters within the ventral and dorsal premotor areas. Subcortical

activations are focused in the posterior thalamus on both sides. A cluster within the right superior cerebellum can also be observed.

The activation patterns obtained by the group level statistical analysis, completely satisfy the expectation of a visually guided reach to grasp task, including the LOC area related to object recognition (Kourtzi & Kanwisher, 2001) as well as other areas involved in visually guided reaching and grasping, for example the aIPS, PMv and PMd; for review see Castiello (2005) and references therein.

5.2.2 Balancing the included trials with regard to a kinematic parameter approach

The results presented below are based on trial balancing prior to fixed and random effect statistical analyses. Two separate grasp components have been chosen as major balancing criteria, namely the response time RT and the overall movement time MT. In our dataset, RT is significantly shorter for Fam objects, while MT is shorter for Geo objects. Both parameters can also be measured without continuous video recording, hence increasing the applicability in different setups.

5.2.2.1 Balancing the included trials with regard to the measured response times

For this analysis familiar and geometric trials have been balanced in respect to the response time shown by the participants. Mean response times were 385ms (Fam) and 401ms (Geo) prior to balancing, $p < 0.001$, and were changed to 388ms (Fam) and 399ms (Geo), $p < 0.01$. Note that there is still a significant difference between the groups. This is a good showcase of a problem associated with trial balancing: it is extremely unlikely to achieve complete accordance of the groups without discarding the majority of the data.

Still, already this subtle shift led to a much more refined activation pattern as compared to the standard approach. Grasping (Fam - Geo), at $p < 0.001$ unc., t

= 3.43 and k = 30, corresponding to $p < 0.05$ corrected (see figure 5), shows relatively large clusters expanding over the postcentral and supramarginal gyrus bilaterally, whereas the left hemisphere one also covers the anterior intraparietal sulcus. On the left we also see activations in the lateral occipital cortex (LOC), ventral premotor cortex (PMv), insular cortex and the rostral middle frontal gyrus (rostral MFG). On the right hemisphere only a small PMv cluster is left behind. Subcortical activations involve the left posterior thalamus.

5.2.2.2 Balancing the included trials with regard to the measured complete movement times

In this case, familiar and geometric trials have been balanced regarding the complete movement time (response to finish). Mean complete movement times have been 2.54s (Fam) and 2.44s (Geo) prior to balancing, $p < 0.001$, and could be moved to 2.45s (Fam) and 2.43s (Geo), $p < 0.01$. Again, there is still a significant difference between the groups, but the shift of the mean difference from almost 100ms to less than 20ms is a massive improvement. Also note that the mean complete movement time for the Geo objects decreased, and not only for the Fam objects. This can be attributed to the fact that both the unusually short and the unusually long movement time trials were removed into the error trial category for both object categories.

The clusters we observed in this analysis (Grasping (Fam - Geo), $p < 0.001$, $t = 3.43$, $k = 31$; equals $p < 0.05$ corrected, see figure 5) covered the postcentral and supramarginal gyrus bilaterally, with the left hemisphere cluster expanding into the anterior intraparietal sulcus. On the left we also see activations in the lateral occipital cortex (LOC), ventral premotor cortex (PMv), insular cortex and the rostral middle frontal gyrus (rostral MFG). Cerebellar activations are bilateral small clusters in the superior part (Lobe VI). No subcortical activations were visible.

In general, the balancing the included trials with regard to either RT or MT, effectively filters the result, as compared to the standard approach. The clusters are a lot more defined, and the general activation pattern compares to the

standard analysis. In both cases, even when balancing based on a single parameter, mean parameter values were still significantly different between grasping Fam and Geo objects. Hence it is futile to balance the trials based on multiple parameters, as it would ideally be the case, and we refer to exploring further options.

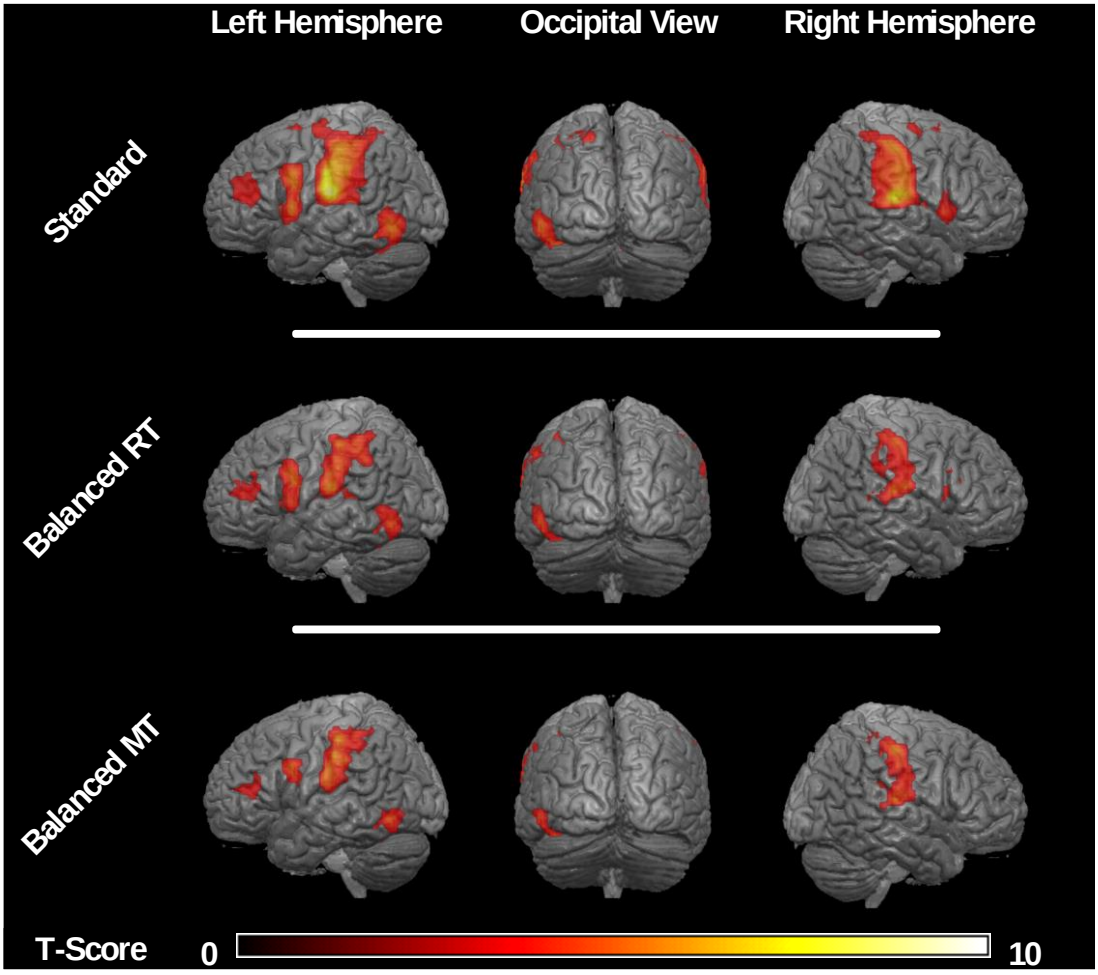

Figure 5:

Significant differences for the main effects comparison of grasping familiar objects minus grasping geometric objects, presented at a cluster-level corrected $p < 0.05$. Displayed are: the standard analysis: upper row. Further analyses included trials that were balanced according to either: response time (balanced RT): middle row; or the complete movement time (balanced MT): lowest row.

5.2.3 Including grasp kinematics as covariates into the random effects analysis

For this analysis, kinematic parameters were taken as covariates into the random effects group analysis. Four different combinations have been explored: response time only, complete movement time only, response time and complete movement time as independent covariates, and all 6 measured movement components as independent covariates. The whole brain t-maps for these analyses are displayed in figure 6.

5.2.3.1 Response time as covariate of no interest.

Detectable activations for Grasping (Fam - Geo), at $p < 0.001$, $t = 3.45$, and $k = 63$; equals $p < 0.05$ corrected, are bilateral clusters covering the postcentral and supramarginal gyrus, on the left hemisphere the anterior inraparietal sulcus (aIPS), the temporoparietal junction (TPJ), the lateral occipital cortex (LOC), the insular cortex, and the ventral premotor cortex (PMv). No subcortical or cerebellar activations were detectable.

5.2.3.2 Total movement time as covariate of no interest.

The evaluated t-map is calculated based on Grasping (Fam - Geo), at $p < 0.001$, $t = 3.45$, and $k = 63$; equalling $p < 0.05$ corrected. On the left hemisphere visible activations include the lateral occipital cortex (LOC), ventral premotor cortex (PMv), the inferior postcentral gyrus the temporoparietal junction (TPJ), and supramarginal gyrus (SMG). Clusters within the anterior insular cortex can be seen bilaterally. On the right hemisphere we see clusters in the PMv and the SMG. No subcortical or cerebellar activations can be detected.

5.2.3.3 Response time and total movement time as covariates of no interest.

The shown activation map is determined via Grasping (Fam - Geo), at $p < 0.001$, $t = 3.47$, and $k = 63$; equalling $p < 0.05$ corrected. Interestingly, only two clusters survived the thresholding. These were located on the supramarginal

gyrus (SMG), the temporoparietal junction (TPJ), and the inferior postcentral gyrus. No subcortical or cerebellar activations can be detected.

5.2.3.4 All six reach to grasp movement components as covariates of no interest.

The displayed activations for Grasping (Fam - Geo), with $p < 0.001$, $t = 3.55$, and $k = 58$; equalling $p < 0.05$ corrected, result from applying response time, response to reach, reach to lift, lift to placement, placement to return onset, and return onset to finish durations as independent covariates. On the left hemisphere visible clusters include the lateral occipital cortex (LOC), the anterior intraparietal sulcus (aIPS), the anterior insula, and the ventral premotor cortex (PMv). A cluster within the anterior cingulate cortex (aCC) was located medially and involves both hemispheres. On the right hemisphere a well-defined cluster within the PMv can be observed. No subcortical or cerebellar activations were evident.

Including kinematic parameters as covariates of no interest into the random effect analysis proves to be an effective way of refining the original analysis results. Using either the response time or the complete movement time leads to a more sufficient cluster size reduction compared to the trial balancing approach, without the serious drawback of having to discard data. Applying both of them leads to a very radical cluster reduction: suppression of meaningful activations seems very likely in this case. When adopting all 6-recorded kinematic parameters as covariates, the result is a reasonable compromise between cluster size reduction, and pattern pervasiveness; this method also makes best use of the level of detail that could be achieved during the kinematics analysis.

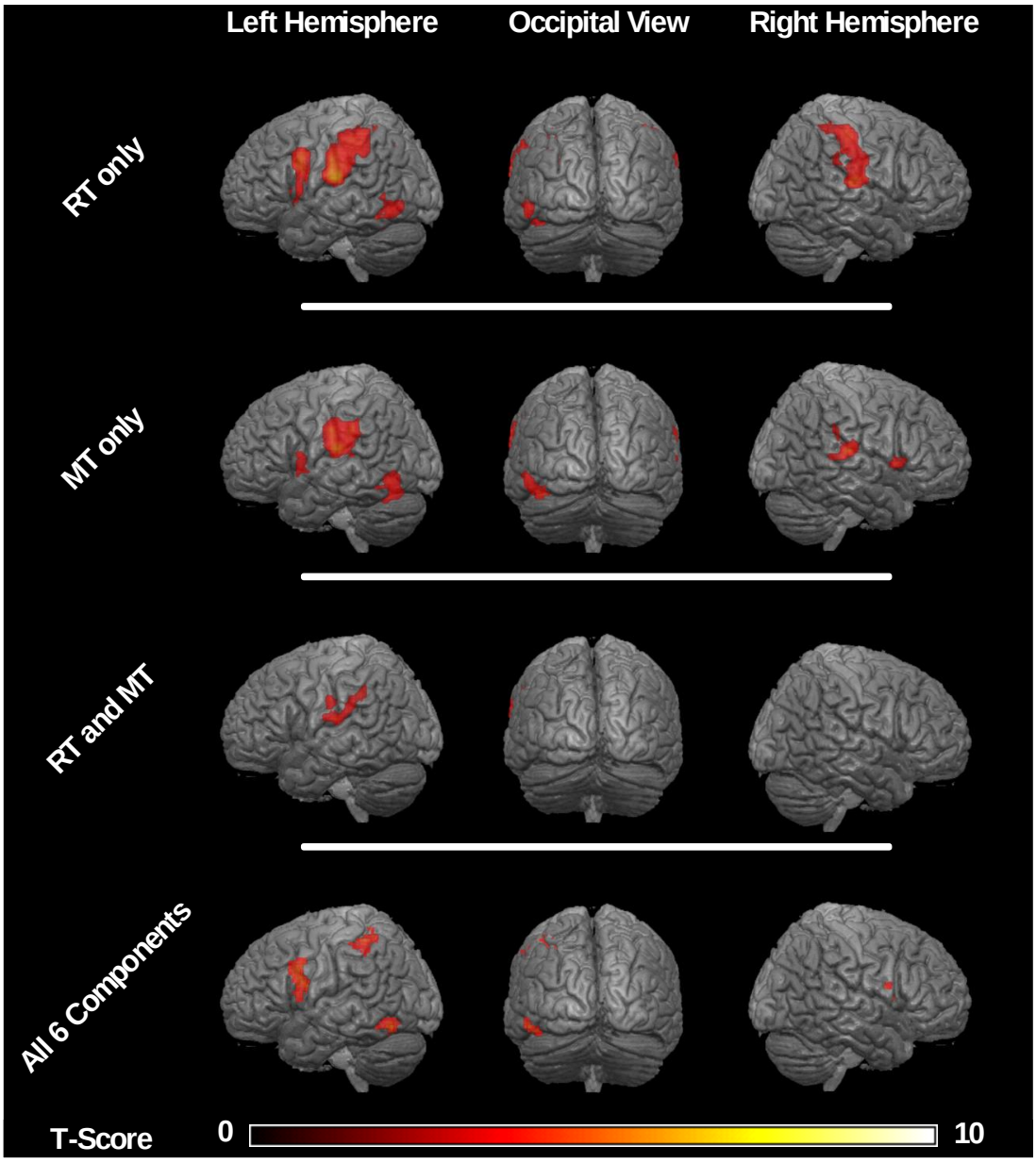

Figure 6:

Covariates of no interest approach; presented are significant differences for the main effects comparison of grasping familiar objects minus grasping geometric objects, at a cluster-level corrected $p < 0.05$.

Displayed are: response time RT as only covariate at group level: upper row. Complete movement time MT as the only covariate at group level: 2nd row from the top. Response time RT and movement time MT as covariates at group level: 3rd row from the top. The analysis including all six movement components as covariates of no interest in the random effects group analysis: lowest row.

5.2.4 Strategy evaluation summary

In the previous sections we have taken a closer look at the durations of different parts of our participants' reach to grasp movements, discovered a difference between the groups of grasped objects (familiar and geometric, see Section 4.1.2) in most of the movement parts (response time, reach to lift, lift to placement, placement to return onset, and complete movement time, i.e. response to finish). We then concluded that these subtle differences might have had an impact on the outcome of the statistical analysis of our functional MRI data, and have investigated several ways to integrate the gathered kinematic data into the statistical analysis, in order to weaken the influence of these potentially confounding factors.

At first, to have a point of comparison, we conducted a ‘standard’ analysis without regard for the measured kinematics. The activation patterns obtained by the group level statistical analysis, completely satisfied the expectancy of a visually guided reach to grasp task, including the lateral occipital cortex area generally related to object recognition (Kourtzi & Kanwisher, 2001) as well as other brain areas involved in visually guided reaching and grasping, like the aIPS, PMv and PMd (Castiello, 2005). However, the clusters involved in the abovementioned pattern are large, and seemingly confluent. It therefore seemed beneficial for a more precise interpretation, to refine the result.

Our next step was therefore an attempt to consider movement kinematics by using them as a reference to balance the trials that would subsequently be analysed within the general linear model at a single subject level. This involved discarding trials with values deviating too far from the mean, on a session by session basis. It could be stated, that balancing the included trials with regard to either reaction time or total movement time effectively filters the result, as compared to the standard approach. The clusters are more defined, with the general activation pattern persisting from the original analysis. Yet, in both cases, even when balancing based on a single parameter, mean parameter values could not be shifted to non-significant

difference levels between grasping familiar and geometric objects without discarding unacceptable amounts of data. Therefore it would have proven ineffective to balance the trials based on multiple parameters, as it would ideally be the case, and we referred to exploring further options.

The next possibility that had been explored involved including kinematic parameters as covariates of no interest into the group random effect analysis. It proved to be an effective way of refining the original analysis results. Using either the response time, or the complete movement time as covariates led to a greater cluster size reduction in comparison to the trial balancing approach, without having to discard data. Applying both of them leads to a very radical cluster reduction: suppression of meaningful activations seemed very likely in this case. When adopting all 6 recorded kinematic parameters as covariates, a method that made maximum use of the level of detail we could acquire, the result was a reasonable compromise between cluster size reduction, and pattern pervasiveness.

Having evaluated different functional analysis options with and without movement kinematics integration we can conclude, that incorporating movement parameters has a substantial effect on the outcome. Taking up kinematic parameters as covariates of no interest into the group level random effect analysis has emerged as a practical and elegant solution. This shows that numerous previous studies addressing cortical grasping control must have yielded at least partially incorrect results, as long as movement kinematics have not been incorporated into the analysis. Based upon this, even beyond the scope of sensomotorics, a very detailed record of the participants' behaviour within an MR setup is certainly advisable.

5.3 FMRI task related activations contrasted to the baseline signal

In the following section we shall take a look at the activation patterns shown during the attentive viewing and grasping tasks, contrasted against the fixation baseline. Contrasting to the baseline leads to these patterns being statistically very powerful and pervasive across the different analysis strategies discussed in the previous section; with the attentive viewing task analysis remaining identical. Based on the conclusion of our strategy evaluation, the analysis including all six movement components as covariates of no interest in the random effects group analysis will form the foundation of all the results presented below. Main effect t-maps are uniformly presented at $p < 0.05$ FWE, and are displayed in figure 7.

5.3.1 FMRI activation patterns shown in the attentive viewing task

Activations shown during the attentive viewing task (voxelwise threshold $p < 0.05$ FWE), both in viewing Fam and Geo, are almost symmetrical; we see a large cluster covering the primary visual cortex (V1) as well as secondary visual cortices (V2, V3), a cluster within the lateral occipital cortex (LOC), posterior superior temporal gyrus, and posterior parts of the intraparietal sulcus can also be seen bilaterally.

By looking at the main effects during the attentive viewing task we could assess brain areas involved in this visual process. Beyond that, this essential contrast serves as a test of result plausibility, and fully satisfied our expectations as such.

5.3.2 FMRI activation patterns shown in the grasping task

Displayed are activations shown during the grasping task contrasted against the baseline with a voxelwise threshold of $p < 0.05$ FWE. In both grasp Fam and grasp Geo, we see large clusters covering the postcentral and supramarginal

gyrus bilaterally, on the left reaching into the precentral gyrus, especially the hand knob (Yousry et al., 1997) area. Also, the supplementary motor area (SMA), the ventral and dorsal premotor cortices (PMv, PMd), the anterior cingulate cortex (ACC) primary and secondary visual cortices (V1, V2, V3), the superior parietal lobe (SPL), the temporoparietal junction (TPJ), the lateral occipital cortex (LOC) and the insular cortex show activation on both hemispheres. Subcortical activations cover the thalamus dorsalis and the lentiform nucleus on both sides. Cerebellar activations are focused in the superior parts (Lobes V-VII).

By looking at the main effects of the reach to grasp trials, we could identify the brain regions involved in the entire sensorimotor process of visually guided grasping, including the occipital, superior parietal, postcentral, precentral, and secondary motor cortices. Their involvement in the task is perfectly plausible based upon existing fundamental studies.

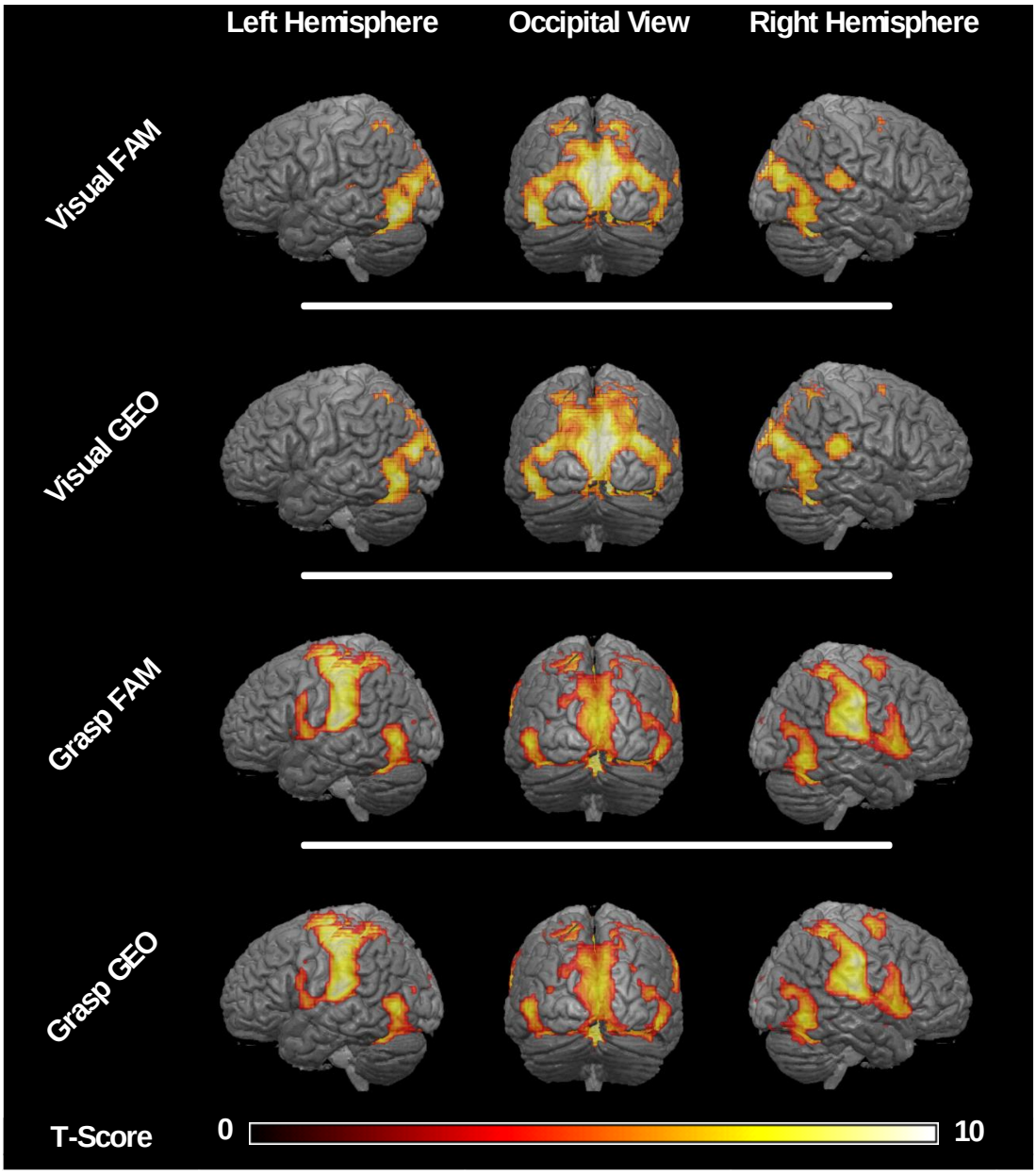

Figure 7:

Shown are significant main effects ($p < 0.05$ FWE) for the conditions FAM and GEO; attentive viewing trials on the upper 2 rows and grasping trials on the lower 2 rows. The cuneus, occipital and lateral occipital areas are shared in both purely visual and grasping tasks, while additional grasp-related motor and somatosensory networks can be observed during grasping only. Note that the activation patterns are grossly similar between the FAM and GEO categories.

5. 4 FMRI signal contrasted between the familiar and geometric categories

5.4.1 Impact of object category on the fMRI response during the attentive viewing task

The pattern revealed to us by calculating the main effects comparison of attentively viewing Fam minus viewing Geo, thresholded at $p < 0.001$ unc., $t = 3.43$, $k = 67$, equal to $p < 0.05$ corrected, consists of a bilateral cluster within the lateral occipital cortex (LOC) region, which is slightly bigger on the left (see figure 8, upper part).

The statistical analysis of attentively viewing familiar versus geometric objects reveals areas of both right and left lateral occipital cortex showing a significantly stronger signal while observing meaningful items rather than abstract shapes. The involvement of the LOC in our attentive viewing task matches well with our expectations of this area playing a vital role in visual object recognition. Whether this area is involved in visually guided reaching to grasp meaningful objects as well, is one of our major questions, and is investigated in the grasping task.

5.4.2 Impact of object category on the fMRI response during the grasping task

The main effect comparison displayed in figure 8, lower part, has been first introduced in our preceding kinematic investigation (see section 5.2.3), i.e. Grasping (Fam - Geo), with $p < 0.001$, $t = 3.55$, and $k = 58$; equalling $p < 0.05$ corrected. On the left hemisphere visible clusters include the lateral occipital cortex (LOC), the anterior intraparietal sulcus (aIPS), the anterior insula, and the ventral premotor cortex (PMv). A cluster within the anterior cingulate cortex (aCC) is located medially and involves both hemispheres. On the right hemisphere a well-defined cluster within the PMv can be observed. No subcortical or cerebellar activations are evident.

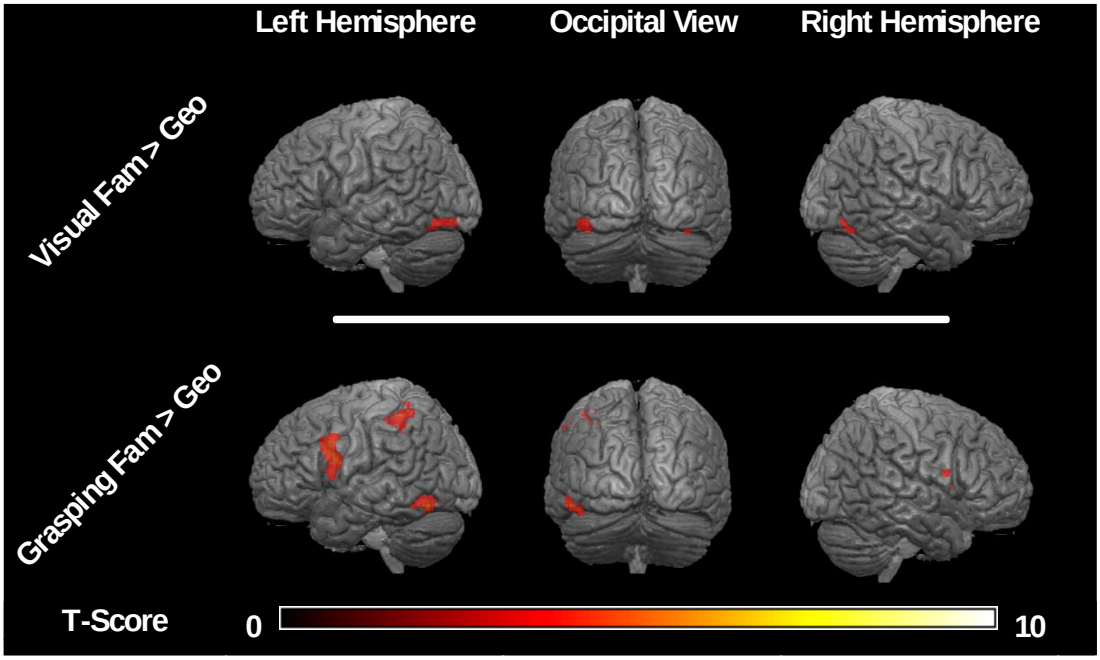

Figure 8:

In the upper part significant differences for the main effects comparison of attentively viewing familiar objects minus attentively viewing geometric objects are presented. Bilaterally areas of the lateral occipital cortex LOC show greater signal during the viewing of the familiar objects. $P < 0.05$ corrected, $k = 66$ voxels.

In the lower part significant differences for the main effects comparison of grasping familiar objects minus grasping geometric objects are displayed. Greater signal during grasping familiar objects is measured in the left lateral occipital cortex LOC, the left anterior part of the intraparietal sulcus aIPS, and the bilateral ventral premotor cortex PMv (with the left PMv cluster being noticeably large than the right). $P < 0.05$ corrected, $k = 58$ voxels.

5.5 A closer look at the object category dependent responses

Percent signal changes (PSCs) have been extracted, as described in section 4.4.5, from the significant cluster peaks introduced in the previous section, see table 2. Statistics that are reported were calculated for the peak PSC using paired T statistic.

Within the grasping trials we can detect a prominently stronger PSC for grasping Fam in all investigated regions of interest (ROIs), including the grasping ROIs, and the lateral occipital cortex (LOC) cluster peaks obtained from the attentive viewing data. The visual ROIs show significantly different signal changes in the left LOC ($p < 0.01$, $t = 3.01$, $df = 26$) and the right LOC ($p < 0.01$, $t = 4.32$, $df = 26$) during the grasping trials (see figure 9 and table 3). Statistical testing for the grasping ROIs was biased, as they were driven by the same dataset, and is therefore refrained from. Within the attentive viewing dataset, of the grasping driven ROIs, only the left LOC shows significant difference between the categories ($p < 0.05$, $t = 2.57$, $df = 26$). Signal change in the visual ROIs is eminently stronger for the Fam objects, but statistical comparison would be meaningless for reasons described above.

Overall, the picture delivered by the region of interest analysis confirmed our impression from the full brain analysis. The grasp associated ROIs, i.e. the left anterior intraparietal sulcus, the left and right ventral premotor cortex, and the anterior cingulate cortex show higher percent signal changes during the grasping trial, and therein a stronger response while grasping familiar objects. More importantly, these ROIs do not show a significant difference during the attentive viewing trials, meaning that they are indeed predominantly active during actual reach to grasp planning. As for the visual associated ROIs (lateral occipital cortex areas from both the grasping and attentive viewing conditions), they show eminently stronger signal increase while either grasping or viewing familiar as opposed to geometric objects.

This is perfectly plausible, as we expect object recognition to play a vital role in both tasks.

By extracting the peak percent signal changes from the significant cluster of our attentive viewing and grasping task we could perform a more detailed, qualitative assessment of the task related MR signal in these regions, in contrast to the almost binary significant-or-no approach characteristic for the whole brain t-maps.

Grasping Conditions	MNI coordinates		
ROI Name	X	Y	Z
left PMv	-42	2	19
left LOC	-51	-64	-14
left aIPS	-45	-43	55
mesial. aCC	0	38	40
right PMv	45	-1	22
Visual Conditions	MNI coordinates		
ROI Name	X	Y	Z
left LOC	-33	-58	-11
right LOC	33	-49	-17

Table 2:

Region of Interest peak MNI coordinates based on significant suprathreshold clusters of the differential analysis of grasping familiar versus geometric objects ('Grasping Conditions', minimal cluster size K = 58 voxels, threshold equal to $p < 0.048$ FWE) and viewing familiar versus geometric objects ('Visual Conditions', minimal cluster size K = 67 voxels, threshold equal to $p < 0.048$ FWE).

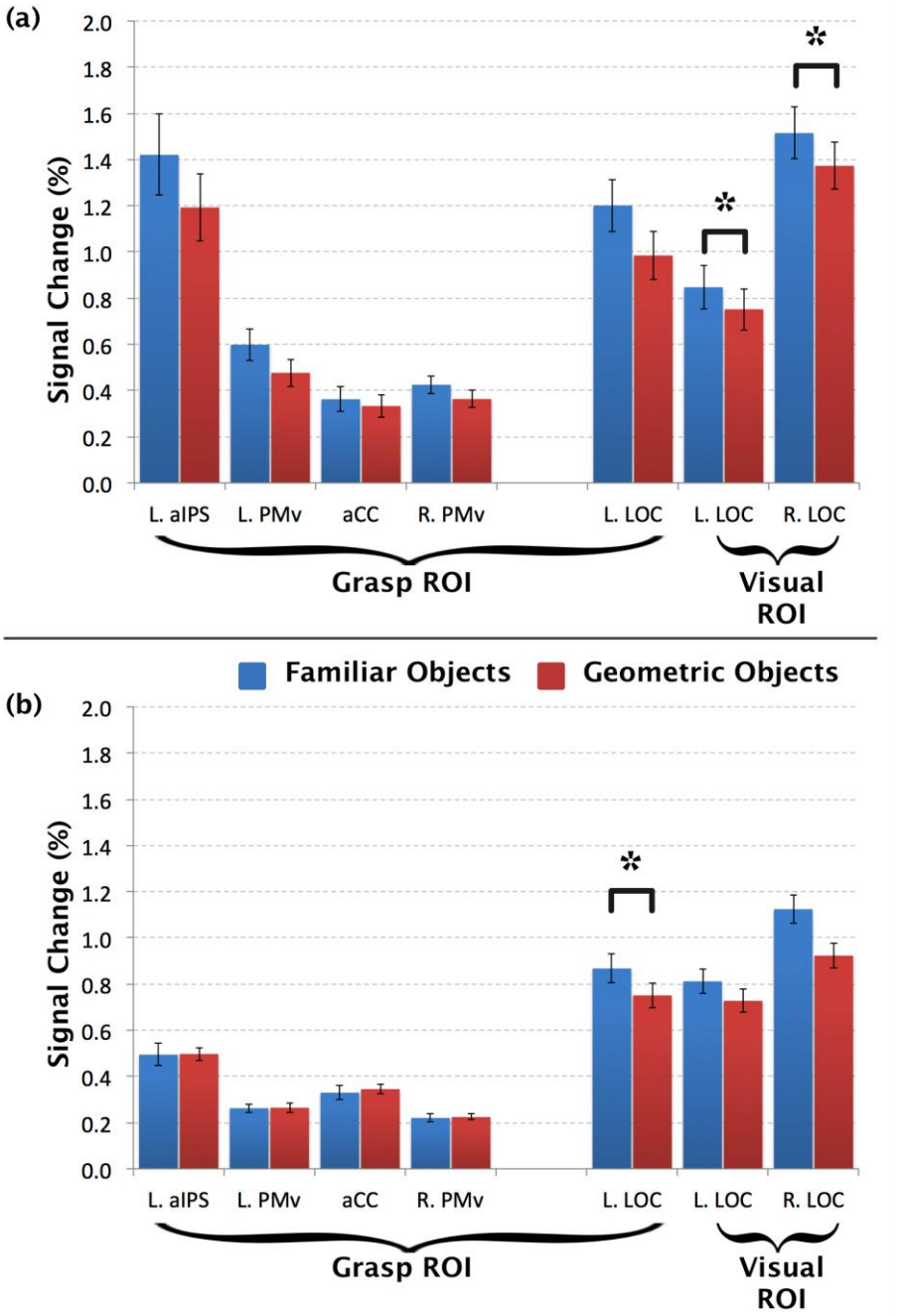

Figure 9:

Displayed are mean ± SEM Percentage Signal Changes for the regions of interest that had a significant difference (cluster-level corrected $p < 0.05$.) in the main effects comparison of Familiar minus Geometric either during grasping (Grasp ROI) or during attentive viewing (Visual ROI).

(a): Percentage Signal Changes during the grasping trials. Only the independently acquired visual ROIs are eligible for statistical testing, and show significant differences between the categories in favor of the familiar objects.

(b): Percentage Signal Changes during the attentive viewing trials. Only the independently acquired grasping ROIs are eligible for statistical testing, and hereof only the left LOC shows a significant difference between the categories.

		ROIs derived from Grasping Conditions					ROIs derived from Visual Conditions	
		L. aIPS	L. PMv	aCC	R. PMv	L. LOC	L. LOC	R. LOC
Grasp Familiar	Mean	1.42	0.60	0.36	0.42	1.20	0.85	1.51
	SEM	0.17	0.07	0.05	0.04	0.11	0.09	0.11
Grasp Geometric	Mean	1.19	0.48	0.33	0.36	0.98	0.75	1.37
	SEM	0.14	0.06	0.05	0.04	0.10	0.09	0.10
	p	< 0.001	< 0.001	0.349	0.001	< 0.001	0.005	< 0.001
Visual Familiar	Mean	0.49	0.26	0.33	0.22	0.87	0.81	1.12
	SEM	0.05	0.02	0.03	0.02	0.06	0.05	0.06
Visual Geometric	Mean	0.50	0.26	0.34	0.22	0.75	0.73	0.92
	SEM	0.03	0.02	0.02	0.01	0.05	0.05	0.05
	p	0.944	0.914	0.518	0.794	0.016	0.002	< 0.001

Table 3:

Percent signal changes in the regions of interest derived from grasping conditions (left part) and attentive viewing conditions (right part) during the planning of reach to grasp movement (upper part) and during the attentive viewing trials (lower part). P values were calculated via a 2-tailed paired t-test for each ROI.

6. Discussion

By using video based recording of hand movements we were able not only to identify correct behavioral responses and exclude incorrect behavioral responses, but also determine basic kinematic parameters for the reach to grasp movements. Finding a significant impact of object familiarity on the durations of certain movement parts, the most prominent example being the faster response time for the meaningful objects, confirms our expectations in the importance of prior object knowledge in human grasping.

We detected the expected signal change differences in the aIPS region, and linked it specifically to visuomotor, and not just purely visual tasks. Hereby a strict control of participant behavior was employed and behavioral differences were implemented into the analysis. This is an important procedure many contemporary studies still do not undertake.

6.1 Kinematics incorporation strategies in fMRI

On the basis of our video assisted study of human reach to grasp movements, we could refine the results of the whole brain statistical analysis by implementing all 6 measured parts of the movement as covariates of no interest into the random effects group level analysis. We stress the importance of accounting for behavioral data in fMRI studies, especially for motor studies. If no account of actual participant behavior is present, it is impossible to appropriately interpret the MR signal. Methods of movement kinematics acquirement and implementation used in other studies are discussed as follows. One possible option is the acquisition of movement kinematics in an independent behavioral control experiment (Cavina-Pratesi et al., 2010). This has the advantage of increased precision and quality of the obtained kinematic data through the use of a dedicated motion capturing system. Such systems cannot be used in the vicinity of or even inside an active MR scanner primarily for safety reasons, because of imaging artifacts, and because of the limited working space. Thus, at first glance an independent behavioural control measurement seems strictly superior to the available procedures within the

scanner bore. However even in setups excellently mimicking the experimental setup within the scanner, kinematic parameters measured this way in the best-case scenario represent merely the typical grasping behavior of the particular participant, and are not directly linked to the cerebral processes inquired upon in the functional imaging investigation. A possible compromise is the use of alternative electronic, but MR compatible movement registration systems, for example with glove based approaches, one possibility being the ShapeClaw System (SouVR Co., Inc, Beijing, China). However, originating in the motion capturing animation industry, such systems are not yet sufficiently established in the scientific context, with absolute finger position measurement errors in the magnitude of 10mm - 20mm (Lawrence et al., 2011). Furthermore, a glove based system influences the grasping hands exteroceptive properties, potentially weakening the experiments external validity with regard to environmental human grasping.

The amount to which kinematic data is analyzed in fMRI reach and grasp studies shows a surprisingly high amount of variation. Some studies even completely omit the acquisition of kinematic data (Konen, Mruczek, Montoya, & Kastner, 2013). Others stop at the point of determining that kinematic differences between multiple categories are non-significant or small (Cavina-Pratesi et al., 2010, 2007). Yet in the context of our findings, the validity of this admittedly simple solution may be doubted. During the course of our kinematic parameter implementation, we could demonstrate that even minimal absolute kinematic differences can yield a massive influence on the outcome of the statistical functional data analysis. A more appropriate option in our eyes is testing, whether the result of the FMRI data analysis can be sufficiently explained by the variance in the kinematic data (Verhagen et al., 2008). If the outcome of this test is negative, we can at least be sure that the overall result cannot be sufficiently explained by the differences in kinematics only. However, parts of the resulting activation pattern could still be substantially influenced by these differences. One important point to be noted about kinematic implementation in general, is that the correlation of kinematics and MR signal change may be indeed have meaningful neurobiological basis, and there is no

known solution to avoid deemphasizing actually meaningful activations in the process.

Overall we can conclude that, when concerning studies of the neuronal basis of human movement, an evaluation of the investigated movement's kinematic parameters is essential. The technical possibilities for assessing kinematics, even within the challenging environment of MRI scanners, will offer options superior to the manual video analysis in the near future. We nevertheless have to point out, that even the most basic and easily measured kinematic parameters, like response time or the complete movement time, contribute considerably to the refinement of the whole brain analysis. Consequently, implementing any kind of measured kinematics into the statistical brain analysis is something we advise strongly. An elegant and powerful solution for this aim with fMRI studies is the employment of kinematic parameters as covariates of no interest in the group level random effect analysis.

6.2 Correlates of object recognition in the human brain

The statistical analysis of attentively viewing familiar versus geometric objects reveals areas of both right and left lateral occipital cortex showing a significantly stronger signal while observing meaningful items rather than abstract shapes. A landmark investigation of the neuroanatomical correlates of object recognition was performed by Pohl (1973); removal of the inferior temporal cortex in rhesus monkeys led to prominent deficits in an object discrimination task. Based on this finding Ungerleider et al. (1998) introduced the model of an occipitotemporal object vision pathway, that has been reinterpreted by Goodale and Milner (1992) as the ventral stream encompassing a perceptual representation of the visual world. Functional imaging of the human inferior temporal cortex has revealed areas responding to certain object categories, for example faces (Puce, Allison, Gore, & McCarthy, 1995), body parts (Taylor, Wiggett, & Downing, 2007) or geographical landmarks (Epstein & Kanwisher, 1998). A contrary view by O'Toole, Jiang, Abdi, and Haxby (2005) suggests, that the ventral temporal cortex is an at least partially distributed network of feature

analyzers (features are defined as shared image-based attributes ,the exact nature of the features is unknown) rather than category modules

Severe disorders of object recognition are known as visual form agnosia (VFA) in humans. Patients with VFA cannot identify or match presented objects based on visual form or orientation cues, while, most notably, visually guided motor tasks are relatively intact (M. a Goodale, Milner, Jakobson, & Carey, 1991). The investigated patient DF could not visually identify everyday objects, geometric shapes and pictures of friends and relatives. However she could accurately reach out and grasp the same objects, appropriately scaling the grip even if the objects were randomly changed during testing (A. D. Milner, Ganel, & Goodale, 2012; Whitwell, David Milner, Cavina-Pratesi, Byrne, & Goodale, 2014). While DFs anatomical MRI showed signs of diffuse hypoxic damage due to carbon monoxide poisoning, she displays apparent focal bilateral lesions within the lateral occipital cortex. In a different case study by Karnath et al. (2009), bilateral lesions of the medial temporal cortex have been reported in a VFA patient with a behavioral deficit profile very similar to patient DF. It is possible that both the lateral and the medial ventral occipitotemporal cortex are vital components of object shape recognition processing. Further evidence for the involvement of the lateral occipital cortex in object recognition is provided by functional imaging studies: several investigations could delineate the lateral occipital cortex as a critical area associated with object recognition (Cavina-Pratesi et al., 2007; James, Culham, Humphrey, Milner, & Goodale, 2003; Kourtzi & Kanwisher, 2001).

At present, a substantial amount of evidence for an object recognition pathway anatomically located in the human lateral occipital and inferior temporal cortex has been collected. Whether as a network of category specific areas or as a distributed network of feature analyzers remains a matter of debate. Either concept matches well with our finding of increased signal in an area of the lateral occipital cortex during attentively viewing familiar versus geometric objects. If we consider the region’s responses in the grasping task, it seems likely that the lateral occipital cortex is the locus involved in familiar object recognition within visually guided grasping as well, potentially contributing

experience based physical object information in the movement planning process.

6.3 The role of brain areas LOC, aIPS and PMv in visually guided grasping

The contrast between grasping familiar and geometric objects revealed brain areas showing a significantly stronger response during the planning of reach to grasp movements towards meaningful everyday items as opposed to meaningless shapes. We could thus identify the anterior intraparietal sulcus aIPS, the ventral premotor cortex PMv and the lateral occipital cortex LOC as areas considerably involved in the integration of prior object knowledge accessible through object recognition into the planning of target-oriented reach to grasp movements. The LOC, as described before, is considered a critical part of the ventral occipito-temporal visual perception stream (M. A. Goodale & Milner, 1992), and is especially relevant for object and form recognition (Cavina-Pratesi et al., 2007; Kourtzi & Kanwisher, 2001). This function is fairly plausible within the context of our study; the LOC could be the brain area contributing grasp relevant object information based on the object identity in the process of visuomotor integration. Both the PMv and the aIPS are part of the dorsal occipito-parietal stream of visual action control (M. A. Goodale & Milner, 1992), more precisely of its dorsolateral portion (Jeannerod, Arbib, Rizzolatti, & Sakata, 1995). The aIPS has been shown to be an important grasp related region. Neuropsychological studies revealed that patients with lesions covering the aIPS contralateral to the grasping hand show impairments of grasping, with the reach movement component still intact (Binkofski et al., 1998). Functional brain imaging studies employing PET and fMRI demonstrate stronger responses in the aIPS region during grasping as compared to reaching (Culham et al., 2003; Toni, Rushworth, & Passingham, 2001). In a purely visual task with 3-dimensional items the aIPS has shown no signal differences among differently sized objects (Cavina-Pratesi et al., 2007). This result contributes to the concept of the aIPS being an actual grasp movement related region rather than an object size analysis module. A dynamic casual modeling study of the

dorsal occipitoparietal pathway demonstrates close functional coupling of PMv to the aIPS during the grasping of small cuboids (Grol et al., 2007). In a transcranial magnetic stimulation experiment Davare, Andres, Cosnard, Thonnard, and Olivier (2006) induced virtual lesions of the PMv contralateral to the grasping hand. This manipulation led to a significantly longer movement and contact time in a grasp and lift task, while also impairing intrinsic hand muscle recruitment determined via electromyography of the abductor pollicis brevis and first dorsal interosseus muscles. The authors therefore postulate that the contralateral PMv is involved in the planning of a precise hand shape and the calculation of the appropriate amount of force during grasping. Shimazu, Maier, Cerri, Kirkwood, and Lemon (2004) demonstrated that direct microelectrode stimulation of the macaque PMv consistently modulated the motor output of the primates' primary motor cortex M1 based on intracellular recordings of upper limb motor neuron electric activity after M1 stimulation. Shimazu et al. (2004) hence concluded that the PMv has robust cortico-cortical connections to the primary motor cortex likely to be relevant in visually guided grasping.

Evidence for an interaction of object recognition in the ventral stream and grasp configuration in the aIPS and the PMv has been collected in an fMRI study by Makuuchi, Someya, Ogawa, & Takayama (2012). Using dynamic casual modeling, the authors could demonstrate increased effective connectivity between the aIPS and posterior inferior temporal gyrus (part of the ventral occipitotemporal pathway) in pantomime tasks involving increased grip selection demands, i.e. pantomimed power grip to objects previously precision gripped and vice versa. The interaction of the aIPS and the PMv with the LOC has also been investigated in an fMRI experiment by Verhagen et al. (2008). During a reach to grasp task towards differently slanted rectangular prisms the 3 regions all showed increased differential responses between monocular and binocular viewing conditions increasing with object slant. Additionally, a psychophysiological interaction analysis procured in the study could detect increased effective connectivity between the aIPS and the LOC, as well as the aIPS and the PMv as a function of object slant during the monocular viewing condition trials. The authors propose that the lateral occipital – dorsolateral

circuit is a processing network for perception based information in the course of visuomotor transformation. This view also makes sense in the context of our study: while grasping meaningful objects, our participants could access prior knowledge about physical object properties via the LOC, and integrate them into the reach to grasp movement planning via the dorsolateral regions aIPS and PMv. This resulted in a faster onset of movement as compared to grasping meaningless geometric shapes. It should be noted that Verhagen et al. (2008) focused on the interaction in the monocular viewing condition, while our investigative focus lies on environmental binocular human grasping.

The existing works provide conclusive evidence for the crucial roles of the aIPS and the PMv in human visually guided grasping. Indications for an interaction between the ventral visual perception stream and these grasp specific areas could also be gathered. This contributes to our interpretation that pre-learned typical object sizes of well-known familiar objects are accessible for the motor system upon object identification. Such object identification makes a significant contribution to the observed signals in the dedicated visuomotor grasping areas PMv and aIPS. Thus, signal processing in these regions is not merely related to purely spatial features of objects but also to non-spatial features that are used for their identification.

7. Conclusions

The current study provides an in-depth look into the difference that accounting for kinematic variables in a reach-to-grasp action can have upon fMRI analysis and its interpretation. Using kinematic parameters as covariates within the analysis at the group level enabled us to control for sources of unwanted variance related to motor behavior; signal clusters obtained using this approach were prominently more delineated as compared to analyses without direct kinematics implementation. The magnitude of this effect shows that numerous studies, which are not accounting for kinematic differences, must come to at least partially incorrect interpretations. Based on the results of this study we would strongly advise the recording and implementation of detailed behavioral information in functional brain imaging studies.

Furthermore, this investigation focuses on visuomotor integration in human grasping. During the grasping of physical objects, brain areas LOC, aIPS and PMv show greater signal change during the planning of reach to grasp actions of meaningful everyday objects as compared to unicolour wooden blocks of similar physical dimensions. During the attentive viewing of these objects, only the brain area LOC displays stronger signal change for familiar everyday objects as compared to similarly sized wooden blocks. Based on these findings, we propose a model, in which prior object knowledge accessible via object recognition in the area LOC, is being provided to the grasp specific brain areas aIPS and PMv in order to facilitate and optimize grasp action planning.

8. References

Bandettini, P. a., & Cox, R. W. (2000). Event-related fMRI contrast when using constant interstimulus interval: Theory and experiment. *Magnetic Resonance in Medicine*, *43*(4), 540–548. doi:10.1002/(SICI)1522-2594(200004)43:4<540::AID-MRM8>3.0.CO;2-R

Bandettini, P. A., Jesmanowicz, A., Wong, E. C., & Hyde, J. S. (1993). Processing strategies for time-course data sets in functional MRI of the human brain. *Magnetic Resonance in Medicine : Official Journal of the Society of Magnetic Resonance in Medicine / Society of Magnetic Resonance in Medicine*, *30*(2), 161–173. doi:10.1002/mrm.1910300204

Binkofski, F., Dohle, C., Posse, S., Stephan, K. M., Hefter, H., Seitz, R. J., & Freund, H. J. (1998). Human anterior intraparietal area subserves prehension: a combined lesion and functional MRI activation study. *Neurology*, *50*(5), 1253–1259. doi:10.1212/WNL.50.5.1253

Birn, R. M., Bandettini, P. a., Cox, R. W., & Shaker, R. (1999). Event-related fMRI of tasks involving brief motion. *Human Brain Mapping*, *7*(2), 106–114. doi:10.1002/(SICI)1097-0193(1999)7:2<106::AID-HBM4>3.0.CO;2-O

Borchers, S., Christensen, A., Ziegler, L., & Himmelbach, M. (2011). Visual action control does not rely on strangers-Effects of pictorial cues under monocular and binocular vision. *Neuropsychologia*, *49*(3), 556–563. doi:10.1016/j.neuropsychologia.2010.12.018

Borchers, S., & Himmelbach, M. (2012). The recognition of everyday objects changes grasp scaling. *Vision Research*, *67*, 8–13. doi:10.1016/j.visres.2012.06.019

Borra, E., Belmalih, A., Gerbella, M., Rozzi, S., & Luppino, G. (2010). Projections of the hand field of the macaque ventral premotor area F5 to the brainstem and spinal cord. *Journal of Comparative Neurology*, *518*(13), 2570–2591. doi:10.1002/cne.22353

Boynton, G. M., Engel, S. a, Glover, G. H., & Heeger, D. J. (1996). Linear systems analysis of functional magnetic resonance imaging in human V1. *The Journal of Neuroscience : The Official Journal of the Society for Neuroscience*, *16*(13), 4207–4221.

Brett, M., Anton, J.-L., Valabregue, R., & Poline, J.-B. (2002). Region of interest analysis using an SPM toolbox. In *8th International Conference on Functional Mapping of the Human Brain*.

Castiello, U. (2005). The neuroscience of grasping. *Nature Reviews. Neuroscience*, *6*(9), 726–736. doi:10.1038/nrn1775

Cavina-Pratesi, C., Goodale, M. a., & Culham, J. C. (2007). FMRI reveals a dissociation between grasping and perceiving the size of real 3D objects. *PLoS ONE*, *2*(5), e424. doi:10.1371/journal.pone.0000424

Cavina-Pratesi, C., Monaco, S., Fattori, P., Galletti, C., McAdam, T. D., Quinlan, D. J., … Culham, J. C. (2010). Functional magnetic resonance imaging reveals the neural substrates of arm transport and grip formation in reach-to-grasp actions in humans. *The Journal of Neuroscience : The Official Journal of the Society for Neuroscience*, *30*(31), 10306–10323. doi:10.1523/JNEUROSCI.2023-10.2010

Culham, J. C., Danckert, S. L., DeSouza, J. F. X., Gati, J. S., Menon, R. S., & Goodale, M. a. (2003). Visually guided grasping produces fMRI activation in dorsal but not ventral stream brain areas. *Experimental Brain Research*, *153*(2), 180–189. doi:10.1007/s00221-003-1591-5

Davare, M., Andres, M., Cosnard, G., Thonnard, J.-L., & Olivier, E. (2006). Dissociating the role of ventral and dorsal premotor cortex in precision grasping. *The Journal of Neuroscience : The Official Journal of the Society for Neuroscience*, *26*(8), 2260–2268. doi:10.1523/JNEUROSCI.3386-05.2006

Davare, M., Kraskov, A., Rothwell, J. C., & Lemon, R. N. (2011). Interactions between areas of the cortical grasping network. *Current Opinion in Neurobiology*, *21*(4), 565–570. doi:10.1016/j.conb.2011.05.021

Dow, B. M. (1974). Functional classes of cells and their laminar distribution in monkey visual cortex. *Journal of Neurophysiology*, *37*(5), 927–946.

Dreher, B., Fukada, Y., & Rodieck, R. W. (1976). Identification, classification and anatomical segregation of cells with X-like and Y-like properties in the lateral geniculate nucleus of old-world primates. *The Journal of Physiology*, *258*(1976), 433–452.

Ebrey, T., & Koutalos, Y. (2001). Vertebrate Photoreceptors. *Progress in Retinal and Eye Research*, *20*(1), 49–94. doi:10.1016/S1350-9462(00)00014-8

Eickhoff, S. B., Stephan, K. E., Mohlberg, H., Grefkes, C., Fink, G. R., Amunts, K., & Zilles, K. (2005). A new SPM toolbox for combining probabilistic cytoarchitectonic maps and functional imaging data. *NeuroImage*, *25*(4), 1325–1335. doi:10.1016/j.neuroimage.2004.12.034

Epstein, R., & Kanwisher, N. (1998). A cortical representation of the local visual environment. *Nature*, *392*(6676), 598–601. doi:10.1038/33402

Fagg, A. H., & Arbib, M. a. (1998). Modeling parietal-premotor interactions in primate control of grasping. *Neural Networks*. Elsevier Sci Ltd. doi:10.1016/S0893-6080(98)00047-1

Farah, M. (2004). *Visual agnosia*.

Friston, K. J., Holmes, a. P., Worsley, K. J., Poline, J.-P., Frith, C. D., & Frackowiak, R. S. J. (1995). Statistical parametric maps in functional imaging: A general linear approach. *Human Brain Mapping*, *2*(4), 189–210. doi:10.1002/hbm.460020402

Friston, K. J., Williams, S., Howard, R., Frackowiak, R. S., & Turner, R. (1996). Movement-related effects in fMRI time-series. *Magnetic Resonance in Medicine : Official Journal of the Society of Magnetic Resonance in Medicine / Society of Magnetic Resonance in Medicine*, *35*(3), 346–355. doi:DOI 10.1002/mrm.1910350312

Goodale, M. a, Milner, a D., Jakobson, L. S., & Carey, D. P. (1991). A neurological dissociation between perceiving objects and grasping them. *Nature*, *349*, 154–156. doi:10.1038/349154a0

Goodale, M. A., Meenan, J. P., Bülthoff, H. H., Nicolle, D. A., Murphy, K. J., & Racicot, C. I. Separate neural pathways for the visual analysis of object shape in perception and prehension., 4 Current biology : CB 604–610 (1994).

Goodale, M. A., & Milner, A. D. (1992). Separate visual pathways for perception and action. *Trends in Neurosciences*, *15*(1), 20–25. doi:10.1016/0166-2236(92)90344-8

Grèzes, J., Armony, J. L., Rowe, J., & Passingham, R. E. (2003). Activations related to “mirror” and “canonical” neurones in the human brain: An fMRI study. *NeuroImage*, *18*(4), 928–937. doi:10.1016/S1053-8119(03)00042-9

Grol, M. J., Majdandzić, J., Stephan, K. E., Verhagen, L., Dijkerman, H. C., Bekkering, H., … Toni, I. (2007). Parieto-frontal connectivity during visually guided grasping. *The Journal of Neuroscience : The Official Journal of the Society for Neuroscience*, *27*(44), 11877–11887. doi:10.1523/JNEUROSCI.3923-07.2007

Grootoonk, S., Hutton, C., Ashburner, J., Howseman, a M., Josephs, O., Rees, G., … Turner, R. (2000). Characterization and correction of interpolation effects in the realignment of fMRI time series. *NeuroImage*, *11*(1), 49–57. doi:10.1006/nimg.1999.0515

Haffenden, A. M., & Goodale, M. a. (2002). Learned perceptual associations influence visuomotor programming under limited conditions: Kinematic

consistency. *Experimental Brain Research*, *147*(4), 485–493. doi:10.1007/s00221-002-1250-2

Halperin, E. C. (2009). *The pornographic anatomy book? The curious tale of the Anatomical Basis of Medical Practice. Academic medicine : journal of the Association of American Medical Colleges* (Vol. 84). doi:10.1097/ACM.0b013e31819391e2

Heeger, D. J., & Ress, D. (2002). What does fMRI tell us about neuronal activity? *Nature Reviews. Neuroscience*, *3*(2), 142–151. doi:10.1038/nrn730

Hendrickson, a E., Hunt, S. P., & Wu, J. Y. (1981). Immunocytochemical localization of glutamic acid decarboxylase in monkey striate cortex. *Nature*, *292*(5824), 605–607.

Humphrey, N. K. (1970). What the frog's eye tells the monkey's brain. *Brain, Behavior and Evolution*, *3*(November), 324–337. doi:10.1109/JRPROC.1959.287207

Jakobson, L. S., Archibald, Y. M., Carey, D. P., & Goodale, M. a. (1991). A kinematic analysis of reaching and grasping movements in a patient recovering from optic ataxia. *Neuropsychologia*, *29*(8), 803–809. doi:10.1016/0028-3932(91)90073-H

James, T. W., Culham, J., Humphrey, G. K., Milner, a. D., & Goodale, M. a. (2003). Ventral occipital lesions impair object recognition but not object-directed grasping: An fMRI study. *Brain*, *126*(Pt 11), 2463–2475. doi:10.1093/brain/awg248

Jeannerod, M. (1986). Mechanisms of visuomotor coordination: a study in normal and brain-damaged subjects. *Neuropsychologia*, *24*(1), 41–78. doi:10.1016/0028-3932(86)90042-4

Jeannerod, M., Arbib, M. a., Rizzolatti, G., & Sakata, H. (1995). Grasping objects: The cortical mechanisms of visuomotor transformation. *Trends in Neurosciences*, *18*(7), 314–320. doi:10.1016/0166-2236(95)93921-J

Jeannerod, M., Decety, J., & Michel, F. (1994). Impairment of grasping movements following a bilateral posterior parietal lesion. *Neuropsychologia*, *32*(4), 369–380. doi:10.1016/0028-3932(94)90084-1

Jonas, T., & Memorial, M. F. (1970). Organization of vertebrate retinas. *Investigative Ophthalmology*, *9*(9), 655–680.

Karnath, H.-O., Rüter, J., Mandler, A., & Himmelbach, M. (2009). The anatomy of object recognition--visual form agnosia caused by medial occipitotemporal stroke. *The Journal of Neuroscience : The Official Journal*

of the Society for Neuroscience, *29*(18), 5854–5862. doi:10.1523/JNEUROSCI.5192-08.2009

Konen, C. S., Mruczek, R. E. B., Montoya, J. L., & Kastner, S. (2013). Functional organization of human posterior parietal cortex: grasping- and reaching-related activations relative to topographically organized cortex. *Journal of Neurophysiology*, *109*(12), 2897–908. doi:10.1152/jn.00657.2012

Kourtzi, Z., & Kanwisher, N. (2001). Human Lateral Occipital Complex Representation of Perceived Object Shape by the Human Lateral Occipital Complex. *Science*, *293*(5534), 1506–1509. doi:10.1126/science.1061133

Kuffler, S. W. (1953). Discharge patterns and functional organization of mammalian retina. *Journal of Neurophysiology*, *16*(1), 37–68.

Lagnado, L., & Baylor, D. (1992). Signal flow in visual transduction. *Neuron*. doi:10.1016/0896-6273(92)90122-T

Lawrence, J. M., Abhari, K., Prime, S. L., Meek, B. P., Desanghere, L., Baugh, L. a, & Marotta, J. J. (2011). A novel integrative method for analyzing eye and hand behaviour during reaching and grasping in an MRI environment. *Behavior Research Methods*, *43*(2), 399–408. doi:10.3758/s13428-011-0067-y

Lennie, P. (1980). Parallel visual pathways: A review. *Vision Research*, *20*(7), 561–594. doi:10.1016/0042-6989(80)90115-7

Leventhal, a G., Rodieck, R. W., & Dreher, B. (1981). Retinal ganglion cell classes in the Old World monkey: morphology and central projections. *Science (New York, N.Y.)*, *213*(4512), 1139–1142.

Livingstone, M. S., & Hubel, D. H. (1984). Specificity of intrinsic connections in primate primary visual cortex. *The Journal of Neuroscience : The Official Journal of the Society for Neuroscience*, *4*(11), 2830–2835.

Livingstone, M. S., & Hubel, D. H. (1988). Segregation of form, color, movement, and depth: anatomy, physiology, and perception. *Science (New York, N.Y.)*, *240*(4853), 740–749. doi:10.1126/science.3283936

Luppino, G., Murata, A., Govoni, P., & Matelli, M. (1999). Largely segregated parietofrontal connections linking rostral intraparietal cortex (areas AIP and VIP) and the ventral premotor cortex (areas F5 and F4). *Experimental Brain Research*, *128*(1-2), 181–187. doi:10.1007/s002210050833

Makuuchi, M., Someya, Y., Ogawa, S., & Takayama, Y. (2012). Hand shape selection in pantomimed grasping: Interaction between the dorsal and the

ventral visual streams and convergence on the ventral premotor area. *Human Brain Mapping*, *33*(8), 1821–1833. doi:10.1002/hbm.21323

Marotta, J. J., & Goodale, M. a. (2001). Role of familiar size in the control of grasping. *Journal of Cognitive Neuroscience*, *13*(1), 8–17. doi:10.1162/089892901564135

Matelli, M., & Luppino, G. (2001). Parietofrontal circuits for action and space perception in the macaque monkey. *NeuroImage*, *14*(1 Pt 2), S27–S32. doi:10.1006/nimg.2001.0835

Maunsell, J. H., Nealey, T. a, & DePriest, D. D. (1990). Magnocellular and parvocellular contributions to responses in the middle temporal visual area (MT) of the macaque monkey. *The Journal of Neuroscience : The Official Journal of the Society for Neuroscience*, *10*(10), 3323–3334.

Mazaika, Hoeft, Glovera, Mazaika, P. K., Hoeft, F., Glover, G. H., & Reiss, A. L. (2009). Methods and Software for fMRI Analysis for Clinical Subjects. *Human Brain Mapping*, 77309. doi:10.1016/S1053-8119(09)70238-1

McIntosh, R. D., & Lashley, G. (2008). Matching boxes: Familiar size influences action programming. *Neuropsychologia*, *46*(9), 2441–2444. doi:10.1016/j.neuropsychologia.2008.03.003

Milner, A. D., Ganel, T., & Goodale, M. a. (2012). Does grasping in patient D.F. depend on vision? *Trends in Cognitive Sciences*, *16*(5), 256–257. doi:10.1016/j.tics.2012.03.004

Milner, A. D., Perrett, D. I., Johnston, R. S., Benson, P. J., Jordan, T. R., Heeley, D. W., … Terazzi, E. Perception and action in “visual form agnosia”., 114 (Pt 1 Brain : a journal of neurology 405–428 (1991).

Mishkin, M., Ungerleider, L. G., & Macko, K. a. (1983). Object vision and spatial vision: Two central pathways. *Trends in Neurosciences*, *6*, 414–417.

Murata, a, Fadiga, L., Fogassi, L., Gallese, V., Raos, V., & Rizzolatti, G. (1997). Object representation in the ventral premotor cortex (area F5) of the monkey. *Journal of Neurophysiology*, *78*(4), 2226–2230.

Murata, a, Gallese, V., Luppino, G., Kaseda, M., & Sakata, H. (2000). Selectivity for the shape, size, and orientation of objects for grasping in neurons of monkey parietal area AIP. *Journal of Neurophysiology*, *83*(5), 2580–2601.

O’Toole, A. J., Jiang, F., Abdi, H., & Haxby, J. V. (2005). Partially distributed representations of objects and faces in ventral temporal cortex. *Journal of Cognitive Neuroscience*, *17*(4), 580–590. doi:10.1167/4.8.903

Ogawa, S., Lee, T. M., Kay, a R., & Tank, D. W. (1990). Brain magnetic resonance imaging with contrast dependent on blood oxygenation. *Proceedings of the National Academy of Sciences of the United States of America*, *87*(24), 9868–9872. doi:10.1073/pnas.87.24.9868

Ogawa, S., Menon, R. S., Tank, D. W., Kim, S. G., Merkle, H., Ellermann, J. M., & Ugurbil, K. (1993). Functional brain mapping by blood oxygenation level-dependent contrast magnetic resonance imaging. A comparison of signal characteristics with a biophysical model. *Biophysical Journal*, *64*(3), 803–812. doi:10.1016/S0006-3495(93)81441-3

Perenin, M. T., & Vighetto, a. (1988). Optic ataxia: a specific disruption in visuomotor mechanisms. I. Different aspects of the deficit in reaching for objects. *Brain : A Journal of Neurology*, *111 (Pt 3*, 643–674. doi:10.1093/brain/111.3.643

Pohl, W. (1973). Dissociation of spatial discrimination deficits following frontal and parietal lesions in monkeys. *Journal of Comparative and Physiological Psychology*, *82*(2), 227–239. doi:10.1037/h0033922

Poustchi-Amin, M., Mirowitz, S. a, Brown, J. J., McKinstry, R. C., & Li, T. (2001). Principles and applications of echo-planar imaging: a review for the general radiologist. *Radiographics : A Review Publication of the Radiological Society of North America, Inc*, *21*(3), 767–779. doi:10.1148/radiographics.21.3.g01ma23767

Puce, a, Allison, T., Gore, J. C., & McCarthy, G. (1995). Face-sensitive regions in human extrastriate cortex studied by functional MRI. *Journal of Neurophysiology*, *74*(3), 1192–1199.

Robson, J. G. (1966). Spatial and Temporal Contrast-Sensitivity Functions of the Visual System. *Journal of the Optical Society of America*, *56*(August), 1141. doi:10.1364/JOSA.56.001141

Schick, F. (2005). Whole-body MRI at high field: Technical limits and clinical potential. *European Radiology*, *15*(5), 946–959. doi:10.1007/s00330-005-2678-0

Schmidt, R. F., Lang, F., & Thews, G. (2007). *Physiologie des Menschen mit Pathophysiologie*. *Book* (Vol. 29.). doi:10.1007/978-3-540-32910-7

Shimazu, H., Maier, M. a, Cerri, G., Kirkwood, P. a, & Lemon, R. N. (2004). Macaque ventral premotor cortex exerts powerful facilitation of motor cortex outputs to upper limb motoneurons. *The Journal of Neuroscience : The Official Journal of the Society for Neuroscience*, *24*(5), 1200–1211. doi:10.1523/JNEUROSCI.4731-03.2004

Sladky, R., Friston, K. J., Tröstl, J., Cunnington, R., Moser, E., & Windischberger, C. (2011). Slice-timing effects and their correction in functional MRI. *NeuroImage*, *58*(2), 588–594. doi:10.1016/j.neuroimage.2011.06.078

Stark, E., Globerson, A., Asher, I., & Abeles, M. (2008). Correlations between groups of premotor neurons carry information about prehension. *The Journal of Neuroscience : The Official Journal of the Society for Neuroscience*, *28*(42), 10618–10630. doi:10.1523/JNEUROSCI.3418-08.2008

Stockman, a, MacLeod, D. I., & Johnson, N. E. (1993). Spectral sensitivities of the human cones. *Journal of the Optical Society of America. A, Optics, Image Science, and Vision*, *10*(12), 2491–2521. doi:10.1364/JOSAA.10.002491

Taylor, J. C., Wiggett, A. J., & Downing, P. E. (2007). Functional MRI analysis of body and body part representations in the extrastriate and fusiform body areas. *Journal of Neurophysiology*, *98*(3), 1626–1633. doi:10.1152/jn.00012.2007

Toni, I., Rushworth, M. F. S., & Passingham, R. E. (2001). Neural correlates of visuomotor associations spatial rules compared with arbitrary rules. *Experimental Brain Research*, *141*(3), 359–369. doi:10.1007/s002210100877

Tootell, R. B., Hamilton, S. L., & Silverman, M. S. (1985). Topography of cytochrome oxidase activity in owl monkey cortex. *The Journal of Neuroscience : The Official Journal of the Society for Neuroscience*, *5*(10), 2786–2800.

Tranchina, D. (1998). The calculus of rod phototransduction. *The Journal of General Physiology*, *111*(1), 3–6. doi:10.1085/jgp.111.1.3

Ungerleider, L. G., Courtney, S. M., & Haxby, J. V. (1998). A neural system for human visual working memory. *Proceedings of the National Academy of Sciences of the United States of America*, *95*, 883–890. doi:10.1073/pnas.95.3.883

Verhagen, L. (2012). *How to grasp a ripe tomato*. Utrecht University.

Verhagen, L., Dijkerman, H. C., Grol, M. J., & Toni, I. (2008). Perceptuo-motor interactions during prehension movements. *The Journal of Neuroscience : The Official Journal of the Society for Neuroscience*, *28*(18), 4726–4735. doi:10.1523/JNEUROSCI.0057-08.2008

Wandell, B. a. (1995). *Foundations of Vision*. *Photochemical photobiological sciences Official journal of the European Photochemistry Association and*

the European Society for Photobiology (Vol. 21). Sinauer Associates. doi:10.1039/c1pp90008k

Wässle, H., & Boycott, B. B. (1991). Functional architecture of the mammalian retina. *Physiological Reviews*, *71*(2), 447–480.

Whitwell, R. L., David Milner, a., Cavina-Pratesi, C., Byrne, C. M., & Goodale, M. a. (2014). DF's visual brain in action: The role of tactile cues. *Neuropsychologia*, *55*, 41–50. doi:10.1016/j.neuropsychologia.2013.11.019

Won, W. J., Lee, M., & Son, J. W. (2008). Implementation of road traffic signs detection based on saliency map model. *IEEE Intelligent Vehicles Symposium, Proceedings*, *14*(4), 542–547. doi:10.1109/IVS.2008.4621144

Young, M. P. (1992). Objective analysis of the topological organization of the primate cortical visual system. *Nature*, *358*(6382), 152–155. doi:10.1038/358152a0

Yousry, T. a., Schmid, U. D., Alkadhi, H., Schmidt, D., Peraud, a., Buettner, a., & Winkler, P. (1997). Localization of the motor hand area to a knob on the precentral gyrus. A new landmark. *Brain*, *120*(1), 141–157. doi:10.1093/brain/120.1.141

Publications

Publication 1:

E. SHEYGAL, J. MARTIN, M. HIMMELBACH. The impact of kinematics on the interpretation of movement studies in fMRI. Program No. 162.02. 2013 Neuroscience Meeting Planner.

San Diego, CA: Society for Neuroscience, 2013. Online.

Publication 2:

J. A. MARTIN, **E. SHEYGAL**, M. HIMMELBACH. The influence of object distinctiveness on reach-to-grasp signals at the human anterior intraparietal sulcus. Program No. 162.11. 2013 Neuroscience Meeting Planner.

San Diego, CA: Society for Neuroscience, 2013. Online.

Erklärungen zum Eigenanteil

Die Konzeption der Studie erfolgte durch Dr. Marc Himmelbach. Die Entwicklung des Setups durch Dr. Jason Anthony Martin und Dr. Marc Himmelbach.

Die fMRT-Messungen wurden von mir gemeinsam mit Dr. Jason Anthony Martin und Dr. Marc Himmelbach durchgeführt.

Die statistische Auswertung führte ich nach Anleitung und unter Betreuung von Dr. Marc Himmelbach gemeinsam mit Dr. Jason Anthony Martin durch.

Ich versichere, das Manuskript selbständig verfasst zu haben und keine weiteren als die von mir angegebenen Quellen verwendet zu haben.

Tübingen, den 21. Mai 2016

Evgeny Sheygal